

The Method of Maximum Power Transmission Efficiency for the Design of Antenna Arrays

WEN GEYI ^{ID} (Fellow, IEEE)

(Invited Paper)

Research Center of Applied Electromagnetics, Nanjing University of Information Science and Technology, Nanjing 210044, China

CORRESPONDING AUTHOR: W. GEYI (e-mail: wgy@nuist.edu.cn)

This work was supported by the National Natural Science Foundation of China under Grant 61971231.

ABSTRACT Various methods have been proposed to control the electromagnetic fields in the near-or far-field region, one of which is to use antenna arrays. This paper reviews a technique, called the method of maximum power transmission efficiency (MMPTE), for the design of antenna arrays and wireless power transmission (WPT) systems. The method is motivated by the fact that all wireless systems aim to maximize the power transmission efficiency (PTE) between the transmitter and receiver and the PTE can thus be considered as a performance index for the design of WPT system and antenna as well. The MMPTE makes use of the PTE as the performance index to be optimized, and reduces a field synthesis problem into a circuit analysis problem, and is therefore easy to master and implement. It overcomes all the challenges associated with conventional array design methods, and is applicable to the design of any type of antenna array in any environment. This paper summarizes the basic theory of MMPTE and demonstrates MMPTE through a number of near- and far-field applications, including focused antennas, smart antennas, shaped beam antennas, end-fire antennas, multi-beam antennas, polarization-reconfigurable antennas, and wireless power transmission systems.

INDEX TERMS Antenna array, wireless power transmission, pattern synthesis, near-field region, far-field region.

I. INTRODUCTION

IN MICROWAVE frequency regime, antenna arrays are often used to realize desired radiation patterns in the far-field region [1], [2]. The conventional methods for antenna pattern synthesis are problem specific and rely on certain simplifications in order to reduce the complexity of the optimization process. Antenna engineers have been facing a number of challenges associated with array designs. For example, the pattern multiplication rule fails and conventional array analysis based on the antenna array factor is no longer valid when the array elements are not identical or its surrounding environment is too complicated or the inter-element spacing is very small. In view of the fact that numerous antenna arrays are to be deployed in next-generation wireless communication systems, a method that can solve the existing challenges associated with conventional array design methods is urgently required.

Some progresses have been made in recent years in order to overcome the above challenges. For example, a field synthesis method based on a prescribed field distribution on a closed surface enclosing the antenna array has been provided in [3]. By minimizing the active power flow of the error field, an optimal or suboptimal distribution of excitations can be obtained. In this paper, we present a systematical review of an optimization technique for the design of antenna arrays and wireless power transmission (WPT) systems which can overcome the aforementioned challenges, called the Method of Maximum Power Transmission Efficiency (MMPTE). In order to achieve a desired field pattern in the near- or far-field region, a performance index (target function) is usually introduced and optimized during the design of antenna. For the design of a wireless system intended either for the transmission of information or power, a natural performance index is the power transmission efficiency (PTE) between the transmitting (Tx)

and receiving (Rx) antennas, which is defined as the ratio of the power delivered to the load of the receiver to the input power of the transmitter. To attain the best possible quality of wireless communication or power transfer, the PTE has to be maximized. Motivated by the fact that all antennas are designed to enhance the PTE for a wireless system, the PTE can thus be considered as a performance index for the design of antennas.

The MMPTE for multiple antenna system was first proposed by the author in 2010 [4], and has evolved into a powerful optimization method that can be used to design antenna arrays to achieve various field patterns, either in the near- or far-field region and in any environment [5]–[31]. Conventional methods of antenna synthesis largely rely on field theory, while the MMPTE reduces the field synthesis problem into a circuit analysis problem so that the circuit theory can be applied to solve the original field problem. This feature of MMPTE makes the design process of antenna array more accessible for those who are not very familiar with electromagnetic (EM) field theory. The circuit parameters can be acquired either by simulation or by measurement, and for this reason, the MMPTE is applicable to any complicated problem. Whenever the design problem cannot be handled by a state-of-the-art computer, one can resort to measurement to obtain the circuit parameters. Another important feature of the MMPTE is that it contains the information of the environment between Tx and Rx arrays, and therefore can be made adaptive to complicated environments, guaranteeing the best possible performance of the antenna array. The MMPTE has been demonstrated to be superior to most existing array design methods in terms of simplicity, applicability, generality and design accuracy. It generates an optimized distribution of excitation (ODE) for the antenna array to assure that the gain of the array is maximized for a fixed array configuration and is equally applicable for both near- and far-field synthesis problems.

Applications of MMPTE and its latest developments are scattered throughout various publications, and its unique value has not been fully recognized by many researchers. The main purpose of this paper is to give a detailed review of the MMPTE covering the basic theory and typical applications. The paper is organized as follows. A comprehensive description of the theory of power transmission between Tx and Rx arrays of a generic WPT system is presented in Section II. The most general expression of the PTE for the WPT system is derived and then optimized, which yields an algebraic eigenvalue equation. The maximum eigenvalue of the eigenvalue equation corresponds to the maximum possible PTE, and the corresponding eigenvector represents the ODE to be applied to the Tx antenna array to achieve the maximum PTE. Section III extends the MMPTE to the WPT system with Rx arrays replaced by a set of volumes or surfaces selected. In these cases, the PTE of the WPT system is defined by the ratio of the weighted sum of the radiated energies in the volumes or the radiated power through the surfaces over the total input power into the

Tx antenna array. Upon optimization, an eigenvalue equation for determining the ODE of the Tx antenna array is obtained. Section IV demonstrates the MMPTE through a number of practical designs in both near- and far-field regions, including focused antennas, smart antennas, shaped beam antennas, end-fire antennas, multi-beam antennas, and polarization-reconfigurable antennas as well as their applications in mobile devices, base stations, implanted devices, microwave hyperthermia, RFID systems, energy harvesting, etc. Section V shows how the MMPTE is applied to the design of WPT systems. Finally, the main features of the MMPTE are summarized in Section VI.

II. THEORY OF MMPTE

The theory of power transmission between two antennas has been investigated by many authors [32]–[39]. For a power transmission system consisting of antenna 1 and 2, the PTE is defined as the ratio of the power received by antenna 2 to the input power of antenna 1, and can be expressed by [4], [5], [32]

$$\text{PTE} = \frac{\left| \int_{S_1 \text{ or } S_2} (\mathbf{E}_1 \times \mathbf{H}_2 - \mathbf{E}_2 \times \mathbf{H}_1) \cdot \mathbf{u}_n dS \right|^2}{4\text{Re} \int_{S_1} (\mathbf{E}_1 \times \bar{\mathbf{H}}_1) \cdot \mathbf{u}_n dS \text{Re} \int_{S_2} (\mathbf{E}_2 \times \bar{\mathbf{H}}_2) \cdot \mathbf{u}_n dS}, \quad (1)$$

where \mathbf{E}_i and \mathbf{H}_i stand for the fields generated by antenna i when antenna $j(j \neq i)$ is receiving; S_i ($i = 1, 2$) denotes the closed surface that encloses antenna i only; the overbar represents the complex conjugate operation; and \mathbf{u}_n is unit outward normal to the surface S_i . The PTE gets maximized if the fields satisfy the conjugate matching conditions $\mathbf{E}_1 = \bar{\mathbf{E}}_2$ and $\mathbf{H}_1 = -\bar{\mathbf{H}}_2$ on the closed surface S_1 or S_2 . Determining \mathbf{E}_i and \mathbf{H}_i with antenna $j(j \neq i)$ in place is not easy. When the two antennas are in the Fresnel region or far-field region of each other, the problem can be simplified by neglecting the reflections between the antennas. In this case, the fields \mathbf{E}_i and \mathbf{H}_i can be obtained by removing the antenna $j(j \neq i)$. For a WPT system consisting of two planar apertures, the optimization of (1) yields an eigenvalue equation. The maximum eigenvalue of the eigenvalue equation gives the maximum PTE and the corresponding eigenvector is the optimized aperture field distribution [34]–[39]. Once the PTE, the transmission distance and the operating frequency are specified, one can increase the aperture size of antenna to meet the specifications. When the Tx and Rx antennas are in the Fresnel region of each other, the optimized aperture field distributions for both Tx and Rx antennas are found to obey a spherical distribution in phase and a Gaussian-like distribution in amplitude. Physically this implies that the Tx and Rx antennas must focus to each other [37].

Realizing the optimized aperture distribution via a single aperture is impossible in most cases. In addition, the optimization of PTE based on (1) gets very complicated when two antennas are in close proximity. To overcome these difficulties, one can consider the power transmission between two antennas from the circuit point of view instead. The circuit theory of power transmission between

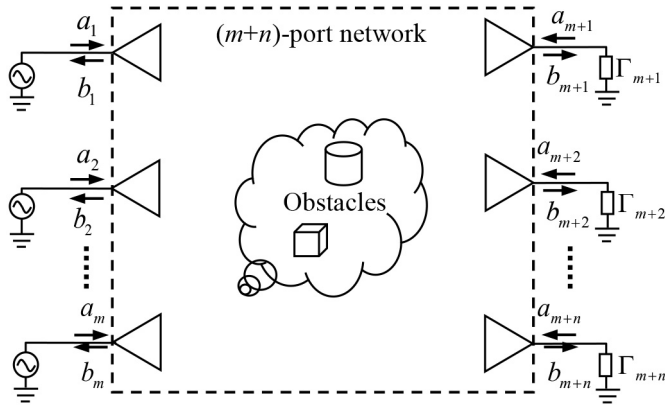


FIGURE 1. A generic WPT system.

two antenna arrays was first investigated in [4]. Consider a generic WPT system located in an arbitrary scattering environment, as illustrated by Fig. 1. The system consists of m Tx antennas and n Rx antennas, and each Rx antenna is terminated by a load of reflection coefficient $\Gamma_i (i = m + 1, m + 2, \dots, m + n)$. The EM waves emanated from the Tx antenna array may bump into a cluster of obstacles and scatterers in the propagation medium and get reflected, refracted and diffracted before they reach the Rx antenna array. The separation between the Tx and Rx antenna arrays is assumed to be arbitrary. The system forms an $(m+n)$ -port network and may be characterized by scattering parameters. The normalized reflective waves and incident waves at the ports are related by

$$\begin{bmatrix} [b_t] \\ [b_r] \end{bmatrix} = \begin{bmatrix} [S_{tt}] & [S_{tr}] \\ [S_{rt}] & [S_{rr}] \end{bmatrix} \begin{bmatrix} [a_t] \\ [a_r] \end{bmatrix}, \quad (2)$$

where

$$[a_t] = [a_1, a_2, \dots, a_m]^T, \quad [b_t] = [b_1, b_2, \dots, b_m]^T$$

are respectively the normalized incident and reflected waves for the Tx array and

$$\begin{aligned} [a_r] &= [a_{m+1}, a_{m+2}, \dots, a_{m+n}]^T, \\ [b_r] &= [b_{m+1}, b_{m+2}, \dots, b_{m+n}]^T \end{aligned}$$

are respectively the normalized incident and reflected waves for the Rx array. The superscript T denotes the transpose operation. For the Rx array, the normalized incident and reflective waves are related by the condition imposed by the loads

$$[a_r] = [\Gamma_L][b_r], \quad (3)$$

where

$$[\Gamma_L] = \text{diag}[\Gamma_{m+1}, \Gamma_{m+2}, \dots, \Gamma_{m+n}]$$

is the load reflection coefficient matrix. Combining (2) and (3) yields

$$\begin{aligned} [b_t] &= [S_{tt}][a_t] + [S_{tr}][\Gamma_L][b_r], \\ [b_r] &= [S_{rt}][a_t] + [S_{rr}][\Gamma_L][b_r]. \end{aligned}$$

By eliminating $[b_r]$ from the first equation, the normalized reflected waves can be expressed in terms of the incident waves $[a_t]$ as follows

$$[b_t] = [\Gamma_{in}][a_t], \quad [b_r] = [T][a_t], \quad (4)$$

where $[\Gamma_{in}]$ and $[T]$ are the input reflection coefficient matrix and the transmission coefficient matrix of the system, respectively given by

$$\begin{aligned} [\Gamma_{in}] &= [S_{tt}] + [S_{tr}][\Gamma_L][T], \\ [T] &= ([1] - [S_{rr}][\Gamma_L])^{-1}[S_{rt}], \end{aligned} \quad (5)$$

and $[1]$ denotes the identity matrix of dimension n . The input power of the WPT system is given by

$$P_{in} = \frac{1}{2} (|[a_t]|^2 - |[b_t]|^2) = \frac{1}{2} [a_t]^H [B] [a_t].$$

where the superscript H denotes the conjugate transpose of matrix, and

$$[B] = [1] - [\Gamma_{in}]^H [\Gamma_{in}], \quad (6)$$

where $[1]$ denotes the identity matrix of dimension m . The received power of the WPT system can be obtained from (3) and the second equation of (4)

$$\begin{aligned} P_{rec} &= \frac{1}{2} (|[b_r]|^2 - |[a_r]|^2) = \frac{1}{2} [b_r]^H ([1] - [\Gamma_L]^H [\Gamma_L]) [b_r] \\ &= \frac{1}{2} [a_t]^H [T]^H ([1] - [\Gamma_L]^H [\Gamma_L]) [T] [a_t] \\ &= \frac{1}{2} [a_t]^H [A] [a_t], \end{aligned}$$

where

$$[A] = [T]^H ([1] - [\Gamma_L]^H [\Gamma_L]) [T].$$

The PTE for the WPT system can then be expressed by

$$\text{PTE} = \frac{P_{rec}}{P_{in}} = \frac{([A][a_t], [a_t])}{([B][a_t], [a_t])}, \quad (7)$$

where (\cdot, \cdot) denotes the usual inner product between two complex column vectors. Equation (7) is a generalized Rayleigh quotient. The PTE (7) can be optimized subject to constraints. Also note that the optimization of (7) is equivalent to optimizing the PTE subject to the constraint that the input power of the WPT system is kept at a constant.

The matrices $[A]$ and $[B]$ are solely determined by the scattering parameters and the load reflection coefficients of the WPT system, and the latter can be obtained either by simulation or by measurement. This flexibility offers great convenience when the system gets too complicated to be modeled by a computer. It is noted that the above derivation is applicable to any WPT system. In other words, the surrounding environment of the system, the separation between the Tx and Rx arrays, the array elements, and the array configuration are all assumed to be arbitrary.

A. UNCONSTRAINED MMPTE

To optimize the PTE expressed by the Rayleigh quotient (7), one can use the variational method. If the quotient (7) is required to be stationary at $[a_t]$, we may obtain the following generalized algebraic eigenvalue equation [4], [5]

$$[A][a_t] = \text{PTE}[B][a_t]. \quad (8)$$

Since both the matrix $[A]$ and $[B]$ are positive, the eigenvalues in (8) are all non-negative. In view of the fact that the number of positive eigenvalues of (8) is equal to the rank of the matrix $[A]$ as well as the following inequality [40]

$$\text{rank}[A] \leq \text{rank}[S_{rr}] \leq \min\{m, n\},$$

the number of positive eigenvalues of (8) is less than or equal to $\min\{m, n\}$. The maximum eigenvalue gives the maximum PTE and the corresponding eigenvector gives the ODE for the Tx array. The eigenvector corresponding to the zero eigenvalue is also useful and it represents the ODE for the Tx array which generates a null in the direction of the Rx array. Based on the ODE, a feeding network for the Tx array can be designed by the theory of transmission line.

Once the ODE for the Tx array is known, the feeding network for the Rx array may be built from the relationship

$$[b_r] = [T][a_t]. \quad (9)$$

The above optimization procedure for the WPT system is called unconstrained MMPTE (UMMPTE) since no essential constraint is involved.

B. WEIGHTED MMPTE

Sometimes constraints have to be imposed to the design of WPT system to realize a specific distribution of the received power among the Rx array elements. To this end, the UMMPTE may be modified by introducing a weighting matrix

$$[W] = \text{diag}[w_{m+1}, w_{m+2}, \dots, w_{m+n}] \quad (10)$$

for the received power $[b_r]$

$$[b'_r] = [W][b_r] = [w_{m+1}b_{m+1}, w_{m+2}b_{m+2}, \dots, w_{m+n}b_{m+n}]^T.$$

Accordingly (7) becomes

$$\text{PTE} = \frac{(|[b'_r]|^2 - |[a_r]|^2)/2}{(|[a_t]|^2 - |[b_t]|^2)/2} = \frac{([A'] [a_t], [a_t])}{([B] [a_t], [a_t])}, \quad (11)$$

where

$$[A'] = [T']^H \left([1] - [\Gamma_L]^H [\Gamma_L] \right) [T']$$

with

$$[T'] = [W][T].$$

Equation (8) is then modified to

$$[A'] [a_t] = \text{PTE}[B][a_t], \quad (12)$$

The MMPTE imposed with the weighting matrix is called weighted MMPTE (WMMPTTE). The above procedure not only achieves the specific distribution of received power but also guarantees that the received power of the Rx array is maximized for fixed input power.

C. CONSTRAINED MMPTE

Different constraints may be enforced on the design of WPT systems. For example, one may require that the received power of the Rx array is equally distributed among its elements

$$|b_{m+1}|^2 = |b_{m+2}|^2 = \dots = |b_{m+n}|^2.$$

In addition to the above constraints, the received power is further required to be maximized. Mathematically one needs to solve a quadratically constrained quadratic programming (QCQP) problem with equality constraints. The solution of this QCQP is not easy [41]–[43]. If the Rx array is in the far-field region and positioned on a sphere centered at the Tx array, the Tx array can then be regarded as a point source. In this case, the phase difference between any two Rx array elements is negligible. Since only the phase differences among the antenna elements are relevant, one may set

$$[S_{rr}][a_t] = [b_r] = [c]e^{j\varphi}, \quad (13)$$

where $[c]$ is an n -dimensional real constant vector, and φ is also a constant phase. Note that the constraint (13) is valid for any distribution of excitations $[a_t]$. We now normalize the denominator of (7) by assuming that $[B] = [1]$ and $([a_t], [a_t]) = [1]$ for simplicity and the QCQP problem may be simplified to a linearly constrained quadratic programming (LCQP) problem as follows

$$\begin{aligned} \max \quad & ([A][a_t], [a_t]) = [a_t]^H [A][a_t] \\ \text{s.t.} \quad & [S_{rr}][a_t] = [c], \end{aligned} \quad (14)$$

where the exponential term $e^{j\varphi}$ in (13) has been factored in the excitation vector $[a_t]$. The problem (14) may be solved by the method of Lagrangian multipliers with a Lagrangian function defined by

$$L([a_t], [\lambda]) = [a_t]^H [A][a_t] - [\lambda]^T ([S_{rr}][a_t] - [c]).$$

The extremum point $([a_t], [\lambda])$ of (14) satisfies the following Lagrangian equations

$$\begin{aligned} \frac{\delta L([a_t], [\lambda])}{\delta [a_t]} &= 2[A][a_t] - [S_{rr}]^H [\lambda] = 0, \\ \frac{\delta L([a_t], [\lambda])}{\delta [\lambda]} &= [S_{rr}][a_t] - [c] = 0, \end{aligned} \quad (15)$$

where $\delta/\delta[a_t]$ and $\delta/\delta[\lambda]$ denote the functional derivatives with respect to $[a_t]$ and $[\lambda]$ respectively. It follows from (15) that the optimized solution of (14) is given by

$$\begin{aligned} [a_t] &= [A]^{-1} [S_{rr}]^H \left([S_{rr}] [A]^{-1} [S_{rr}]^H \right)^{-1} [c], \\ [\lambda] &= 2 \left([S_{rr}] [A]^{-1} [S_{rr}]^H \right)^{-1} [c]. \end{aligned} \quad (16)$$

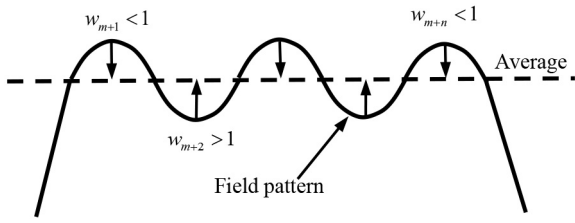


FIGURE 2. Selection of weighting coefficients.

If the Rx array is located in the near-field region of the Tx array, one cannot ignore the phase differences among the Rx elements. If one still follows the above procedure in this case, the distribution of the received power along the Rx array will no longer be flat. Instead, it will oscillate around a constant (the average distribution) with peaks and troughs. To avoid solving the QCQP problem directly, a weighting matrix $[W]$ as defined by (10) may be introduced to bring the peaks and troughs back to their average. The weighting matrix can be determined by simulations. The weighting coefficients must be less than one for the Rx elements at the peaks and larger than one for the troughs, as illustrated in Fig. 2. A few iterations may be needed in order to finalize the weighting matrix $[W]$. We may replace the constant vector $[c]$ in (14) with a new weighted vector $[W][c]$ to solve a new weighted LCQP problem expressed by

$$\begin{aligned} \max \quad & [a_t]^H [A] [a_t] \\ \text{s.t.} \quad & [S_{rt}] [a_t] = [W][c]. \end{aligned} \quad (17)$$

The solution of (17) is then given by

$$\begin{aligned} [a_t] &= [A]^{-1} [S_{rt}]^H \left([S_{rt}] [A]^{-1} [S_{rt}]^H \right)^{-1} [W][c], \\ [\lambda] &= 2 \left([S_{rt}] [A]^{-1} [S_{rt}]^H \right)^{-1} [W][c]. \end{aligned} \quad (18)$$

The MMPTE imposed with the linear constraints is called constrained MMPTE (CMMPTTE). Compared with the UMMPTTE and WMMPTTE, the optimal solution from the CMMPTTE can be determined analytically.

III. EXTENDED MMPTE

The MMPTE discussed in previous Section is based on the circuit theory for a multiport network where both Tx and Rx arrays are involved. One can also get rid of the Rx arrays and introduce other performance indices to achieve various field patterns.

A. ANTENNA ARRAY WITH SPECIFIED ENERGY DISTRIBUTION

If the transmitting antenna is required to focus the EM field energy to multiple regions designated by $\Omega_p (p = 1, 2, \dots, n)$ as illustrated in Fig. 3, we may introduce the ratio of the weighted sum of the radiated energies in the regions $\Omega_p (p = 1, 2, \dots, n)$ over the total input power into the transmitting array as the performance index

$$\text{PTE} = \frac{\sum_{p=1}^n \int_{\Omega_p} W_p(\mathbf{r}) |\mathbf{E}(\mathbf{r})|^2 d\Omega(\mathbf{r})}{P_{in}}, \quad (19)$$

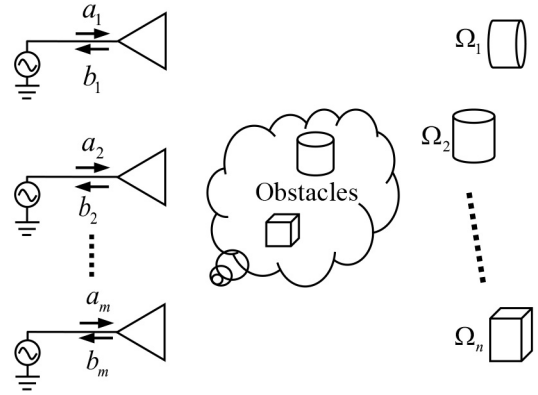


FIGURE 3. An extended WPT system for specified energy distribution.

where $W_p (p = 1, 2, \dots, n)$ are weighting functions that regulate the energy distribution among the designated regions $\Omega_p (p = 1, 2, \dots, n)$. It is noted that one can make the ratio (19) dimensionless by properly selecting the weighting functions although this may not be necessary. Assuming that the transmitting array is well matched, the fields radiated from the transmitting antenna array can then be written as

$$\mathbf{E}(\mathbf{r}) = \sum_{j=1}^m a_j \mathbf{E}_j(\mathbf{r}), \quad \mathbf{H}(\mathbf{r}) = \sum_{j=1}^m a_j \mathbf{H}_j(\mathbf{r}), \quad (20)$$

where $\mathbf{E}_j(\mathbf{r})$ and $\mathbf{H}_j(\mathbf{r})$ are the fields generated by the j th antenna element of the transmitting array when the j th element is excited by $a_j = 1$ and the rest are terminated in a matched load, i.e., $a_i = 0 (i \neq j)$. Thus we may write

$$\begin{aligned} \int_{\Omega_p} W_p(\mathbf{r}) |\mathbf{E}(\mathbf{r})|^2 d\Omega(\mathbf{r}) &= \sum_{i=1}^m \bar{a}_i \sum_{j=1}^m a_j \int_{\Omega_p} W_p(\mathbf{r}) \mathbf{E}_j(\mathbf{r}) \\ &\quad \cdot \bar{\mathbf{E}}_i(\mathbf{r}) d\Omega(\mathbf{r}) \\ &= ([A^p] [a_t], [a_t]) \end{aligned}$$

where $[A^p]$ is an $m \times m$ matrix with the (i, j) elements given by

$$A_{ij}^p = \int_{\Omega_p} W_p(\mathbf{r}) \mathbf{E}_j(\mathbf{r}) \cdot \bar{\mathbf{E}}_i(\mathbf{r}) d\Omega(\mathbf{r}). \quad (21)$$

If the transmitting antenna elements are all matched, we have $P_{in} = ([a_t], [a_t])/2$, and (19) can thus be written as

$$\text{PTE} = \frac{\sum_{p=1}^n ([A^p] [a_t], [a_t])}{([a_t], [a_t])/2} = \frac{([A] [a_t], [a_t])}{([a_t], [a_t])}, \quad (22)$$

with $[A] = 2 \sum_{p=1}^n [A^p]$. Similarly the optimized solution of (22) for the transmitting antenna array can be determined by the eigenvalue equation (8) with $[B]$ set to the identity matrix. The transmitting antenna array excited by the ODE obtained from maximizing (22) focuses the EM field energy to the multiple target regions designated by $\Omega_p (p = 1, 2, \dots, n)$ with a desired energy distribution controlled by the weighting functions. Especially if the weighting functions are selected as $W_p = w_p \delta(\mathbf{r} - \mathbf{r}_p)$ ($p = 1, 2, \dots, n$), the optimization of (22) gives the ODE

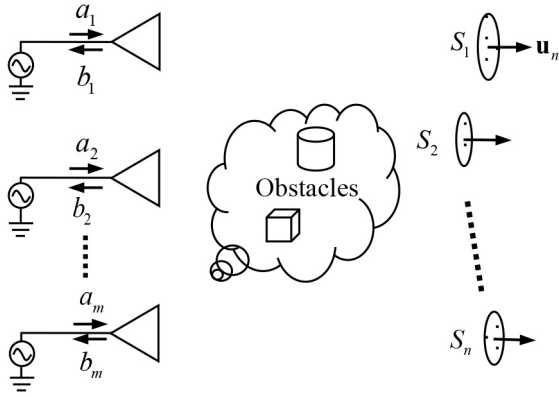


FIGURE 4. An extended WPT system for specified power distribution.

for the transmitting antenna array focused on multiple points $\mathbf{r}_p (p = 1, 2, \dots, n)$. The above strategy can be used to design focused antenna array, smart antenna array, and multi-beam antenna array.

One can also introduce the ratio of the total energy absorbed in the region $\sum_{p=1}^l \Omega_p (l < n)$ over that absorbed in the region $\sum_{p=l+1}^n \Omega_p (l < n)$ as the performance index

$$\text{PTE} = \frac{\sum_{p=1}^l \int_{\Omega_p} W_p(\mathbf{r}) |\mathbf{E}(\mathbf{r})|^2 d\Omega(\mathbf{r})}{\sum_{p=l+1}^n \int_{\Omega_p} W_p(\mathbf{r}) |\mathbf{E}(\mathbf{r})|^2 d\Omega(\mathbf{r})}. \quad (23)$$

Inserting (20) into (23) leads to

$$\text{PTE} = \frac{([A][a_t], [a_t])}{([B][a_t], [a_t])}, \quad (24)$$

where

$$[A] = \sum_{p=1}^l [A^p], \quad [B] = \sum_{p=l+1}^n [A^p].$$

The optimized solution of (24) can be determined by the eigenvalue equation (8). An optimization criterion similar to (23) was introduced to find the optimal excitations for the multi-antenna applicators in regional hyperthermia [44], [45].

B. ANTENNA ARRAYS WITH SPECIFIED POWER DISTRIBUTION

Let $S_p (p = 1, 2, \dots, n)$ denote the surface elements located in various directions as illustrated in Fig. 4. One can introduce the performance index

$$\text{PTE} = \frac{\sum_{p=1}^n \int_{S_p} W_p(\mathbf{r}) \frac{1}{2} \text{Re} \mathbf{E}(\mathbf{r}) \times \bar{\mathbf{H}}(\mathbf{r}) \cdot \mathbf{u}_n dS(\mathbf{r})}{P_{in}}, \quad (25)$$

which is the ratio of the weighted sum of the radiated power in the directions specified by $S_p (p = 1, 2, \dots, n)$ over the total input power into the transmitting antenna array. In the above, $W_p(\mathbf{r}) (p = 1, 2, \dots, n)$ are the weighting functions that regulate the power distribution in the directions designated by $S_p (p = 1, 2, \dots, n)$ and \mathbf{u}_n is the unit normal

vector to the surface element. Taking (20) into account, we may write

$$\begin{aligned} & \int_{S_p} W_p(\mathbf{r}) \frac{1}{2} \text{Re} \mathbf{E}(\mathbf{r}) \times \bar{\mathbf{H}}(\mathbf{r}) \cdot \mathbf{u}_n dS(\mathbf{r}) \\ &= \frac{1}{2} \text{Re} \sum_{i=1}^m \bar{a}_i \sum_{j=1}^m a_j \int_{S_p} W_p(\mathbf{r}) \mathbf{E}_j(\mathbf{r}) \times \bar{\mathbf{H}}_i(\mathbf{r}) \cdot \mathbf{u}_n dS(\mathbf{r}) \\ &= \frac{1}{2} \text{Re} ([A^p][a_t], [a_t]), \end{aligned}$$

where $[A^p]$ is an $m \times m$ matrix with the elements given by

$$A_{ij}^p = \int_{S_p} W_p(r) \mathbf{E}_j(\mathbf{r}) \times \bar{\mathbf{H}}_i(\mathbf{r}) \cdot \mathbf{u}_n dS(\mathbf{r}). \quad (26)$$

If the transmitting antenna elements are all matched, (25) can thus be expressed by

$$\text{PTE} = \text{Re} \frac{([A][a_t], [a_t])}{([a_t], [a_t])} = \frac{([A_c][a_t], [a_t])}{([a_t], [a_t])}, \quad (27)$$

with $[A] = \sum_{p=1}^n [A^p]$ and $[A_c] = \frac{1}{2}([A] + [A]^H)$. The above strategy can be applied to the design of focused antenna array, smart antenna array, and multi-beam antenna array.

Similar to (23), one can also introduce the ratio of the total power radiated in the directions S_1, S_2, \dots, S_l over that radiated in the directions $S_{l+1}, S_{l+2}, \dots, S_n$ as the performance index

$$\text{PTE} = \frac{\sum_{p=1}^l \int_{S_p} W_p(\mathbf{r}) \frac{1}{2} \text{Re} \mathbf{E}(\mathbf{r}) \times \bar{\mathbf{H}}(\mathbf{r}) \cdot \mathbf{u}_n dS(\mathbf{r})}{\sum_{p=l+1}^n \int_{S_p} W_p(\mathbf{r}) \frac{1}{2} \text{Re} \mathbf{E}(\mathbf{r}) \times \bar{\mathbf{H}}(\mathbf{r}) \cdot \mathbf{u}_n dS(\mathbf{r})}. \quad (28)$$

Introducing (20) into (28) yields

$$\text{PTE} = \frac{\text{Re}([A][a_t], [a_t])}{\text{Re}([B][a_t], [a_t])} = \frac{([A_c][a_t], [a_t])}{([B_c][a_t], [a_t])}, \quad (29)$$

where

$$\begin{aligned} [A] &= \sum_{p=1}^l [A^p], \quad [A_c] = \frac{1}{2}([A] + [A]^H), \\ [B] &= \sum_{p=l+1}^n [A^p], \quad [B_c] = \frac{1}{2}([B] + [B]^H), \end{aligned}$$

and the matrix elements of $[A^p]$ are given by (26).

For most applications, such as the design of focused antenna array, smart antenna array and multi-beam antenna, it has been verified that the extended MMPTE without using the test receiving antennas yields results comparable with MMPTE. The extended MMPTE is based on a pure field formulation, whose application studies are still ongoing and will be published in the future. For the above reasons, we will concentrate on the MMPTE and its applications in the following.

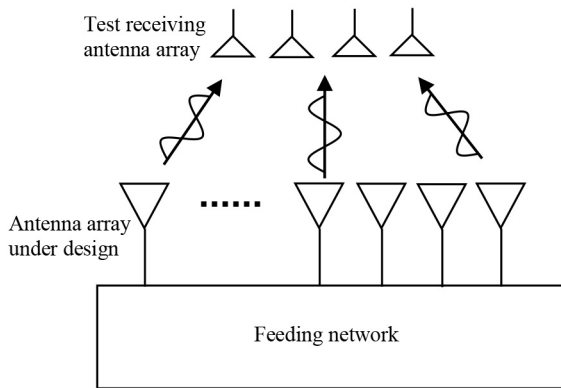


FIGURE 5. Design of antenna array with test receiving antennas.

IV. OPTIMAL DESIGN OF ANTENNA ARRAYS FOR NEAR- AND FAR-FIELD APPLICATIONS

Since the final goal of antenna design is to maximize the PTE between the Tx and Rx antennas, the MMPTE can also be applied to the design of antenna arrays. In fact, the PTE may be used as a performance index or an objective function to be optimized for all antenna designs. For this purpose, the array under design may be set as the Tx and a test array may be introduced and set as the Rx so that they form a WPT system, as illustrated in Fig. 5. Therefore, by properly introducing a test Rx array, the optimal design of an antenna array is transformed into the optimal design of a WPT system and the best possible antenna performance is guaranteed. Different from the design of WPT system, the Rx array introduced in the design of an antenna array is a virtual tool set for determining the scattering parameters and achieving the prescribed field pattern. There is no need to fabricate it eventually.

The design of antenna array for applications in far- or near-field regions can be accomplished in terms of MMPTE by following the same procedures listed below:

- 1) Set up the WPT system: A WPT system may be set up by assuming that the array under design is used as Tx and a test array is introduced as Rx. The type and the number of the test Rx elements and their configuration depend on the field pattern to be realized on the Rx side. The polarization of the test Rx array elements must match that of the Tx array elements. For example, the design of multi-beam antennas requires a test Rx array with its elements being positioned in the directions where the beam needs to be generated.
- 2) Determine the scattering parameters of the WPT system: The scattering parameters of the WPT system can be acquired by simulation or by measurement if the surrounding environment is too complicated or unknown.
- 3) Find the ODE for the array: The ODE can be obtained from (8), (12), (16) or (18), depending on which formulation of MMPTE is used.
- 4) Design the feeding network: Based on the ODE, a feeding network can be designed by the theory of

transmission line. The power dividers in the feeding networks control the amplitude distribution of the excitations while the lengths of the feeding lines control the phase distribution of excitations. The feeding network can also be realized by attenuators and phase shifters available in the market. The excitations with negligible amplitudes in the ODE can be ignored to reduce the number of array elements and simplify the design of the feeding network.

The scattering parameters in MMPTE contain information about the environment between the Tx and Rx arrays and can be obtained by measurement in real time. This is convenient for the design of antennas in a changing environment. For example, the targeted hyperthermia treatment requires accurate knowledge of the electrical properties of the human body, which are usually acquired at the diagnostic stage through medical imaging. In hyperthermia treatment, the patient and properties of the body tissues may change. In these cases, an adaptive approach in real time for hyperthermia treatment is in high demand.

Typically the MMPTE can be applied to the design of focused antenna arrays, smart (beam steering) antenna arrays, end-fire antenna arrays, multi-beam antenna arrays, and the shaped beam antenna arrays. By introducing a single test Rx antenna in the direction where the radiation intensity needs to be maximized or minimized, the UMMPTe (where only one positive eigenvalue is involved) can be used to design the focused antennas [11]–[17], smart antennas [18]–[21], end-fire antennas [24], [25], and polarization-reconfigurable antennas. By introducing a test Rx array, the CMMPTe and WMMPTe (where multiple positive eigenvalues are involved) can be used to shape beam patterns [22], [23], and design antenna arrays with multiple focal points [17], and multiple beam antennas [26], [27].

In recent years, near-field communication (NFC) has found wide application. Understanding the behavior of fields near a radiator and being able to control them are extremely helpful in designing NFC devices. The MMPTE is applicable to the design of antenna arrays in the near- or far-field region and the design procedures are exactly the same.

A. FOCUSED ANTENNA ARRAYS

EM field focusing is required in areas where a high power density must be applied, such as noncontact microwave sensing [46], radiometric temperature sensors [47], microwave hyperthermia [48]–[51], and radio frequency identification (RFID) [52]–[55]. Conventional design methods for the focused antenna array assume a quadratic phase distribution with constant amplitude distribution, which may yield high sidelobes at the focal plane [56]–[57]. Quadratic phase distribution combined with Dolph-Chebyshev amplitude distribution can be used to improve the sidelobes [58]. Another interesting method for focusing EM wave is based on the time reversal (TR) technique [59]–[61], which was first used in acoustics [62].

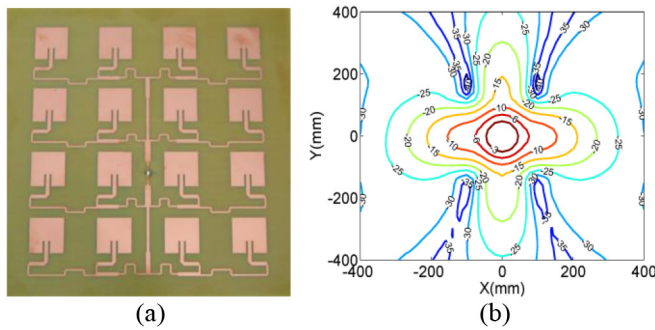


FIGURE 6. (a) Linearly-polarized focused array. (b) Contour plot of the electric field at the focal plane.

Physically focusing the EM energy to a spot (the focal point) by an antenna array is equivalent to delivering the maximum possible power from the array to a test antenna located at the focal point so that the radiated energies from all the array elements converge to the focal point. For this reason, the PTE is an ideal performance index for the design of focused antenna array. For an antenna array with multiple focal points, a testing Rx antenna array may be introduced with its elements placed at the focal points. The eigenvector corresponding to the maximum PTE, obtained from equation (8) or (18), represents the ODE for the focused antenna array and the best focusing performance is guaranteed. Based on the above procedure, different types of focused antenna arrays have been designed for various applications.

1) LINEARLY-POLARIZED FOCUSED ANTENNA ARRAYS [11], [12]

The focused antennas have been investigated for a long time and mainly concentrated on linearly-polarized antenna arrays. A 16-element array operating at 2.45GHz, using a rectangular microstrip patch element with an inset-feed, is designed by UMMPTe in [11]. The array is built on FR4 substrate with relative dielectric constant 4.4, loss tangent 0.02 and thickness of 3mm, as shown in Fig. 6(a). The feeding network is designed in terms of the ODE obtained from (8) with a linearly-polarized testing antenna placed 150mm away from the array along its center axis. It is found that the ODE has a spherical phase distribution and a Gaussian-like amplitude distribution, which is similar to the optimized solution for a continuous aperture [37]. The ODE ensures that the fields generated by the array elements add in phase at the focal point, and the electric fields at the focal plane have no sidelobes. The contour plot of the electric field at the focal plane indicates that the -3dB beam contour has good circular symmetry, indicating that most of the power is concentrated in the middle of the focal plane (see Fig. 6(b)).

The antenna array and the feeding network can be built on the different sides of substrate by introducing a common ground plane in between the array and the feeding

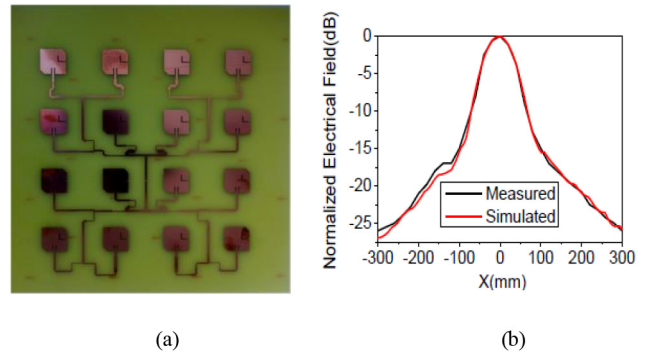


FIGURE 7. (a) CP focused antenna array in a square shape. (b) Normalized electric field distribution at the focal plane.

network [12]. The latter arrangement is better suited for large-scale arrays and is less vulnerable to the environments.

2) CIRCULARLY-POLARIZED FOCUSED ANTENNA ARRAYS [13], [14]

A circularly-polarized (CP) wave has outstanding capability of anti-interference, which motivates the study of CP focused antenna arrays. The design of CP focused antenna array seem more challenging since the distribution of excitation for the antenna array not only determines the focusing properties but also affects the axial ratio (AR) of the antenna array. Two different CP focused antenna arrays, one in a square shape and the other in a ring shape, operating at 2.45GHz, are designed with UMMPTe in [13], [14], and they are built on FR4 substrate. The array element is a rectangular patch with an L-shaped slot for creating a pair of orthogonal modes and two triangles removed from the two corners to further improve the CP performance. A CP patch is used as the test Rx antenna and placed 100 mm away from the array. Again, no sidelobes occur at the focal plane, which indicates that the radiated energy from the array is concentrated around the focal point as illustrated in Fig. 7.

3) FOCUSED ANTENNA ARRAYS FOR MEDICAL APPLICATIONS [15], [16]

The MPMTE can be applied to the design of focused antennas in more complicated environments, such as for microwave hyperthermia, where the influence of human body tissues must be taken into account in the design of antenna arrays [15], [16]. An 18-element focused hexagonal patch array operating at 433MHz, is designed under the load of a body-mimicking phantom by UMMPTe in [16], as illustrated in Fig. 8. The array is built on the FR4 substrate. To reduce the size of the array, a pair of slots are introduced in the rectangular patch element. The patch array and the feeding network are separated by a common ground plane. The body-mimicking phantom and the matching material are prepared and are placed in a cylindrical glass tank. The focal position can be adjusted in real time in the body-mimicking phantom by changing the feeding schemes determined by the ODEs.

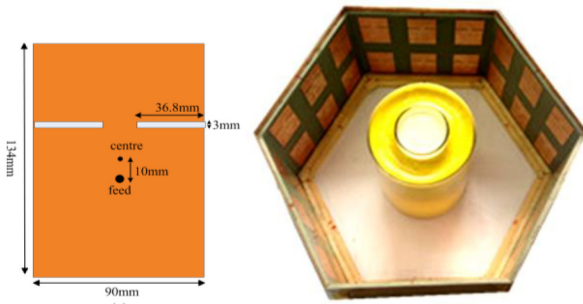


FIGURE 8. Focused hexagonal patch array.

Another interesting application of focused antenna is to wirelessly power implantable devices, which is often accomplished by near-field inductive coupling or non-radiating WPT [63]–[65]. The UMMPTe has been successfully applied to design a focused antenna to power an implantable device in the radiating near-field region [30].

4) ANTENNA ARRAYS WITH MULTIPLE FOCAL POINTS [17]

In some circumstances, a prescribed power distribution among multiple focal points may be required to achieve, for example, simultaneous wireless power transmission (SWPT) to different devices with different input power levels. The proper feeding schemes for SWPT may be obtained by various optimization algorithms such as the Levenberg-Marquardt algorithm [66], [67] and artificial neural networks [68], which seem to be very time-consuming if the number of antenna elements is large. An alternative to realize SWPT is to use the TR method [69]–[71]. Several TR focusing fields inside a closed metal cavity have been achieved with the synthesized distributions of excitations [72]. For most SWPT scenarios, the transmitters and receivers are deployed in an open space, instead of in a closed metal cavity. An algorithm for the synthesis of the near-field pattern in open space is proposed in [73], in which the phase distribution is realized by a coding metasurface, but this algorithm requires huge computational time due to massive source phases.

Two antenna arrays operating at 2.45GHz have been designed in [17] by CMMPTe to focus the EM field energy to multiple targets in both closed and open regions, as shown in Fig. 9(a) and (b). In the design process, the test Rx array elements are divided into two sets. One set denotes the test elements whose received power must be maximized and the other set the test elements whose received power must be minimized. The number of focal points and the power intensity at each focal point are all manageable by regulating the weighting matrix. As a demonstration, the X-shaped, Y-shaped and L-shaped focusing field patterns are achieved in both closed and open regions and are shown in Fig. 9(c).

Compared with other existing methods for the design of focused antenna arrays, the MMPTE features that the field distribution at the focal plane has no sidelobes as the exact

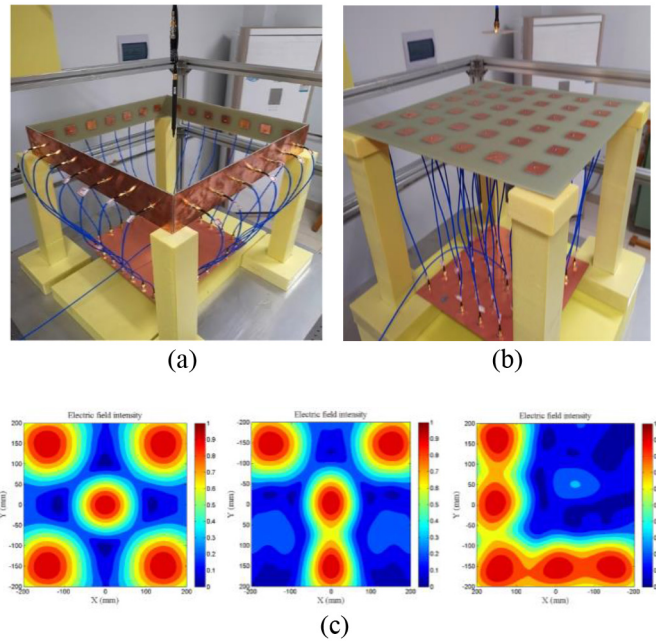


FIGURE 9. Antenna arrays with multiple focal points. (a) Closed region. (b) Open region. (c) Focused field patterns.

theory for a continuous aperture predicts [37]. In addition, the realized focal point is closer to the targeted one.

B. SMART ANTENNAS (BEAM-STEERING ANTENNAS)

Smart antennas have been used in radar system for many years [74], [75], and have recently received increased interest in mobile communication systems for their capability in improving channel capacity and spectrum efficiency, extending coverage, enhancing data rate, steering multiple beams to track many mobiles, and improving service quality [76], [77].

Smart antennas can be categorized as either switched-beam array system or adaptive array system. A switched-beam array system selects one of the predefined beam patterns and changes one beam to another as the mobile user moves around. An adaptive array system optimizes its beam patterns adaptively in response to the signal environment, directs the main beam towards the signal of interest and suppresses the radiation in the direction of interference. Moreover, it largely relies on the signal processing algorithms such as the multiple signal classification algorithm for the estimation of the direction of arrival of the signal and the least mean square algorithm for beamforming.

The MMPTE can be used to determine the distribution of excitations for a smart antenna array to steer the main beam or a null in the desired directions and to ensure that the array gain is optimized. A test Rx antenna may be introduced in the desired direction and placed in the far-field region of the smart array to be designed. The smart array and the test Rx antenna constitute a WPT system. By optimizing the PTE of the WPT system, the ODEs for the smart array can be

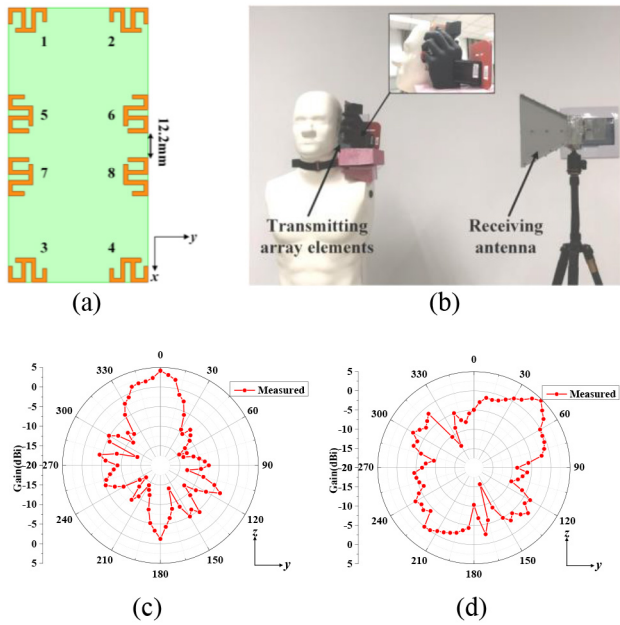


FIGURE 10. (a) 8-element array. (b) Measurement system with a human phantom. (c) Beam directed to positive z-direction. (d) Beam directed to 45° elevation.

determined and be used to generate the main beam or a null in the desired directions.

1) SMART ANTENNAS FOR HANDHELD APPLICATIONS [18], [19]

The smart antenna design for handheld devices has been a challenge for years due to its small size and the complexity of the mobile environments. The MMPTE is capable of solving this problem [18], [19].

A new MIMO (multi-input and multi-output) beam-steering antenna array for a compact and thin handheld device is demonstrated in [18], in which the beam-steering function is enabled for transmitting while the MIMO function for receiving. The MIMO beam-steering antenna array consists of eight printed planar inverted-F elements operating at GSM1900 and LTE2300, as illustrated in Fig. 10(a). A test Rx antenna is introduced in the desired direction, and the UMPTE is then applied to the WPT system consisting of the 8-element array and the test Rx antenna to find the ODE. The simulation and experiments show that the radiation of the antenna array is greatly enhanced in the desired directions and the maximum gain reaches 7.7 dBi.

In practice, the environments, such as the LCD, battery, and other components inside the mobile handsets, have significant impact on the antenna performance. A practical design must consider all these factors, which is difficult to handle even with a state-of-the-art computer. Therefore, the measurement has to be used to attack the problem. A human body phantom is introduced to show how the influence of environments can be determined in [18], as illustrated in Fig. 10(b). A measurement system is set up with a human phantom in place to simulate the phone operation in talking

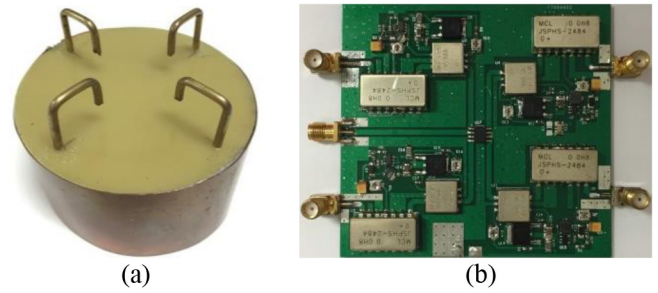


FIGURE 11. (a) Folded monopole array. (b) Feeding circuit board.

position. The eight-element antenna array is held by a hand model and placed near a head model and is set as the Tx antenna while a horn antenna is set as the Rx antenna of the WPT system. The scattering parameters of the WPT system are acquired by a network analyzer which connects the Tx array and the Rx horn placed in the direction in which the radiation intensity is to be enhanced. Once the scattering parameters in the desired direction are determined, the ODE can be obtained from (8). Due to the influence of the phantom, the realized gain is 2 to 3 dB lower than in free space. Fig. 10(c) and (d) show the beam patterns in the desired directions at 2.45GHz.

2) SMART ANTENNAS FOR BASE STATION APPLICATIONS [20], [21]

Customer-premises equipment (CPE) refers to equipment that is located at a subscriber's premises and is connected with a carrier's telecommunication channel. In many situations, the CPE must be "smart" enough to be able to steer the beam towards the desired direction for enhancing the performance of wireless communications. Smart antenna with two radiation modes for CPE applications must have compact size, low cost and beam steering capability in the azimuth plane [78]–[80]. One radiation mode has omnidirectional coverage in the azimuth plane to search for the sources while the other mode has the directional radiation to communicate with high gain and high data-rate.

A 4-element folded monopole antenna array, operating at 2.45GHz, for CPE application is designed by UMPTE in [20]. The folded monopole and the sleeve ground form a quasi-balanced radiating structure, as illustrated in Fig. 11(a). When the amplitudes and phases at the four feeding ports are uniform, the radiation pattern is omnidirectional and the measured gain for the omni-directional pattern is 1.7 dBi. The directional radiation patterns in the desired directions are formed by the ODEs obtained from UMPTE. Fig. 11(b) is the feeding circuit board designed to realize the ODEs. The measured gain for directional pattern is 6.7dBi.

To further reduce the height and improve the front-to-back ratio in the directional mode, two novel dual-mode beam-steerable antenna arrays using arc-shaped dipoles are studied by UMPTE in [21]. Both arrays operate at 2.45GHz and have 360° beam scanning capability in azimuth when

operating in the directional mode. The first array consists of a circular ring reflector and four arc-shaped half-wavelength dipoles with omnidirectional gain of 1.5 dBi, and the peak gain and front-to-back ratio being 7.4 dBi and 15.5 dB respectively in the directional mode. The second array uses the first array as the antenna subarray. Two subarrays form an eight-element array separated by a distance of 0.4 wavelength and placed coaxially with one rotated 45° around the center axis. The second array has a higher omnidirectional gain of 2.9 dBi, and more uniform gain distribution in azimuth in the directional mode, with a peak gain of 8.4 dBi and a front-to-back ratio of 12.5 dB.

It is noted that the signal models used in conventional beamforming algorithms often ignore the mutual couplings among the array elements and the complicated environments [76]. The MMPTE has however incorporated all these factors in the formulation and guarantees that the highest possible gain is achieved in the desired direction.

C. SHAPED BEAM ANTENNA ARRAYS

Radiation patterns with desired shapes can be realized by controlling the distribution of excitations for the antenna arrays. Various optimization methods have been proposed to determine the amplitude and phase distributions for the antenna arrays to achieve a prescribed field pattern in the far-field region [81]–[98]. Various performance indices can be used in pattern synthesis, such as pattern shape, sidelobe levels, front-to-back ratio and gain. It is noted that the desired performance may be unattainable for fixed antenna geometries [99]. The traditional methods of Dolph-Chebyshev, Taylor-Kaiser, Schelkunoff, Fourier transform, and Woodward-Lawson [100], [101], as well as other global optimization methods such as particle swarm optimization [102] and genetic algorithm [103], [104] have found applications in far-field pattern synthesis problems. All these optimization methods are based on the array factor, and they fail whenever the array factor is not available.

In contrast to the sophisticated synthesis methods in the far-field region, only a few methods are available to synthesize a desired pattern in the near-field region [105]–[109]. Most studies are computationally cumbersome since the desired radiation pattern is synthesized on the basis of the radiations of array elements, which needs to be done element-by-element. They are not only complicated, but also inaccurate when the antenna is required to operate in a complicated environment such as inside a metal enclosure.

The MMPTE solves all the challenges associated with the conventional pattern synthesis methods, and is superior to them in many ways. The MMPTE avoids the long searching process in conventional optimization algorithms and can be used to shape beam patterns in both near- and far-field regions as well as in material bodies. According to the beam shape to be realized, a test Rx array may be introduced with its elements properly positioned (see Fig. 12) and weighted as described in WMPTE and CMMPTTE.

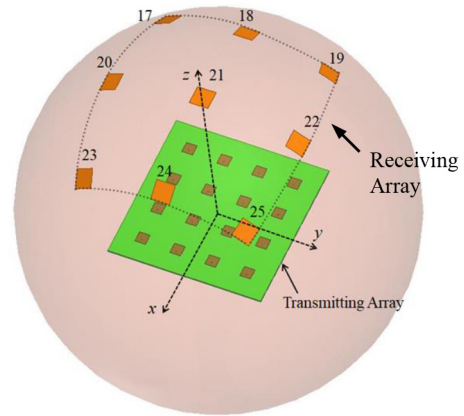


FIGURE 12. Shaped-beam antenna array.

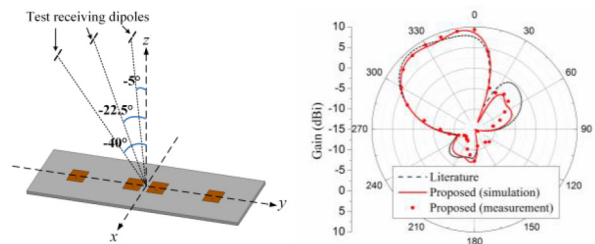


FIGURE 13. (a) Beam shaping antenna array and test receiving dipoles. (b) Radiation patterns of proposed array at 5.4 GHz on yz-plane.

1) BEAM SHAPING IN FREE SPACE [22]

An unequally spaced 4-element patch array is investigated in [22], where array elements and inter-element spacing are selected as in [97] for convenience of comparison. Three test Rx dipoles are positioned on a sphere to achieve a flat-top radiation pattern with 45° covering range for the base station application. The four patch elements and three test Rx dipoles form a seven-port WPT system, as shown in Fig. 13(a). The scattering parameters of the whole system is obtained by simulation tools. The ODE is obtained by CMMPTTE and then realized by a feeding network to produce the desired off-center flat-top radiation pattern shown in Fig. 13(b). The optimized excitation for one of the ports is found to be nearly zero, and can thus be ignored. The optimized solution from CMMPTTE is quite different from the distribution of excitation obtained in [97], in which all the element play the same role and cannot be ignored. Therefore, the MMPTE is able to address the sparse array design by simply discarding those array elements with negligible feeding amplitudes in the ODE.

Fig. 14(a) shows an 8-element array for generating a flat top radiation pattern of square shape in the far-field region, and Fig. 14(b) is the feeding network with 8 feeding ports, which is designed according to the ODE determined from CMMPTTE. The 8-element array is obtained by discarding those elements with negligible amplitudes of excitations from a regular square array originally having 16 elements.

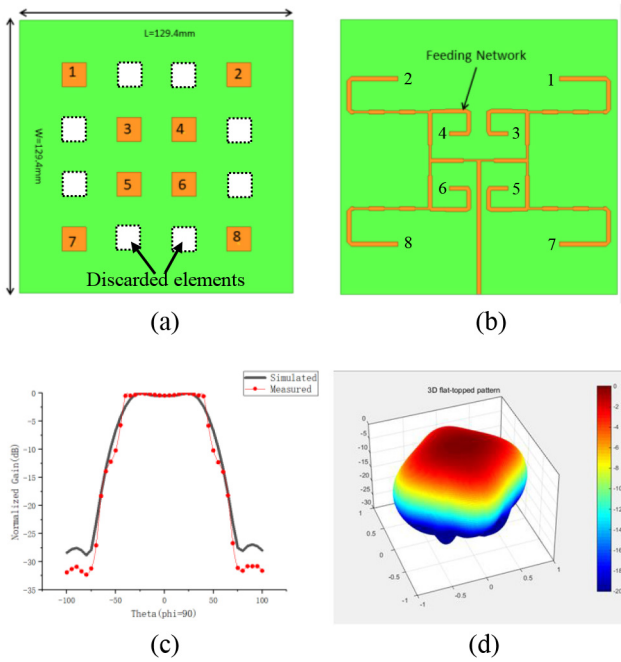


FIGURE 14. (a) Antenna array. (b) Feeding network. (c) 2-D flat top radiation pattern. (d) 3-D square flat top radiation pattern.

Fig. 14(c) and (d) are the 2-D and 3-D shaped radiation patterns. It can be seen that field drops quickly off the flat top region and the measured side lobe levels are below -30dB . In order to generate the desired square flat top radiation pattern, nine test receiving antennas are used and placed on a sphere in the far-field region and arranged as a square shape, as illustrated in Fig. 12.

2) BEAM SHAPING IN A BOOKSHELF ENVIRONMENT [22]

Most reader antennas for library applications are designed in free space without considering the influences of the surrounding books. The CMMPTTE has been applied to the design of a 5-element RFID reader antenna array, operating at 922.5 MHz , for a smart bookshelf of 730 mm in width [22]. The dimensions of the five-element reader antenna array are $730\text{ mm} \times 250\text{ mm} \times 5\text{ mm}$. In order to achieve a flat field pattern across the bookshelf, eleven test Rx antennas are positioned in a row with equal spacing inside a book model of dimensions $850\text{ mm} \times 176\text{ mm} \times 250\text{ mm}$ whose dielectric constant and loss tangent change with frequency, as illustrated in Fig. 15(a). The five-element reader antenna array and the eleven test Rx antennas constitute a sixteen-port network. The ODE for the reader antenna array is obtained from (16) through properly selecting the weighting matrix to generate a flat top radiation pattern inside the book model with the coverage measured at 3 dB being exactly 730 mm . The electric field intensity drops abruptly on both left and right side of the bookshelf, which is enabled by placing the outermost test Rx antennas right above the edge of the reader antenna. The rapid cut-off of the field intensity is helpful in reducing the probability of

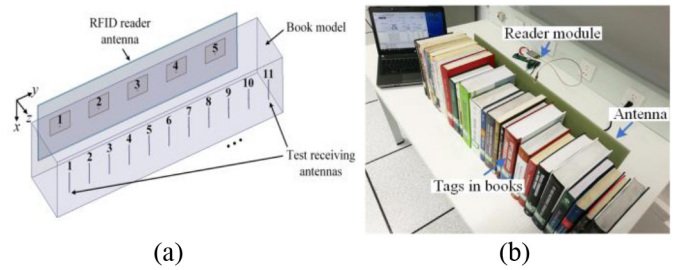


FIGURE 15. (a) Setup for test Rx array. (b). Experimental test system for reader antenna array.

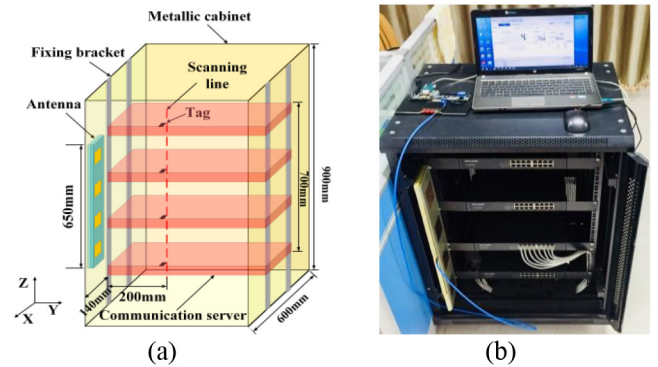


FIGURE 16. (a) A smart telecommunication cabinet. (b) RFID testing system.

misreading the books on the adjacent bookshelf. Fig. 15(b) is the experimental testing system for the reader antenna array.

Many previously reported RFID reader antennas for near-field applications suffer from large fluctuations in field distribution. As a result, the input power may not meet the demands in the lowest electric field areas and may thus cause reading failures. In contrast, the reader antenna designed by the CMMPTTE guarantees the reading accuracy for its wide and flat field distribution which is also optimally enhanced in the reading area.

3) BEAM SHAPING IN A METAL CABINET ENVIRONMENT [23]

A cabinet-level RFID solution for the management of communication servers is proposed in [23]. The reader antenna monitors the servers in a metal cabinet by the tags attached to the servers. The tags are arranged vertically along a straight scanning line, which is 200 mm away from the array and 140 mm away from the front side of the metal cabinet as illustrated in Fig. 16(a). The reader antenna is placed along the edge of the left side of the cabinet for reducing the space occupied by the antenna. The dimensions of the cabinet are $600\text{ mm} \times 600\text{ mm} \times 900\text{ mm}$. The communication servers are placed longitudinally in the cabinet with maximum extension height less than 700 mm . Therefore, it is required that the tracking range of the antenna in the vertical direction of the cabinet is not less than 700 mm .

A four-element patch array, operating at 900 MHz , arranged in the vertical direction is introduced to meet the coverage requirement of the cabinet in the near-field region.

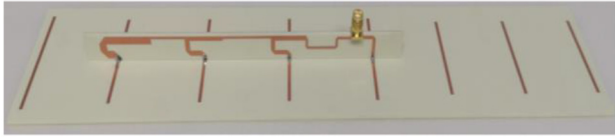


FIGURE 17. Generalized Yagi-Uda dipole antenna.

The antenna elements are printed on top of the first substrate of dimensions $650 \text{ mm} \times 120 \text{ mm} \times 3 \text{ mm}$, while the feeding network is printed on the bottom side of the second substrate of dimensions $650 \text{ mm} \times 120 \text{ mm} \times 1.6 \text{ mm}$, both sharing the same ground. To ensure that the array has no dead zone in the identification area, the electric field distribution in the target identification area must be uniform. To this end, four test Rx dipole antennas positioned along the scanning line are introduced. The four-element patch array and the four test dipoles constitute a WPT system. The four-element array excited with the ODE from CMMPTTE has a uniform field distribution with less than 1.5dBi variation across the scanning line with the length of 710 mm, which is significantly lower than previously reported. Fig. 16(b) shows the RFID testing system.

D. END-FIRE ANTENNA ARRAYS [24], [25]

Yagi-Uda antenna is one of the widely used end-fire antennas, typically consisting of one driven element, one reflector, and several directors [110]–[117]. To design an end-fire antenna array in terms of MMPTE, one can introduce a test Rx antenna in the end-fire direction so that a WPT system can be formed together with the end-fire antenna under design. The ODE for the array can be obtained from MMPTE, and a feeding network can then be built from the ODE to achieve the end-fire function.

A novel design for end-fire antenna is proposed in [24], in which the conventional Yagi-Uda antenna is generalized by introducing multiple driven elements. The ODE for the driven elements is obtained from UMMPTTE, and the end-fire gain of the array is considerably improved, while the number of elements and the longitudinal dimension of the array are substantially reduced in comparison with the conventional Yagi-Uda antenna with a single driven element. Two different arrays are designed in [24]. The first design operates at 5.5GHz and uses split-ring resonator (SRR) as radiating element. Compared to the similar planar SRR Yagi-Uda antenna arrays previously reported [118], the number of antenna elements is reduced from fifteen to eight and the longitudinal dimension is reduced by 46%. The same performances are maintained by using five driven elements, and the gain reaches 11.7 dBi. In the second design, eight printed half-wavelength elements are used, as shown in Fig. 17. With four driven elements, the peak gain reaches 13.4 dBi at 2.45 GHz, which is 1.8 dB higher than the conventional printed Yagi-Uda dipole antenna array with the same number of elements.

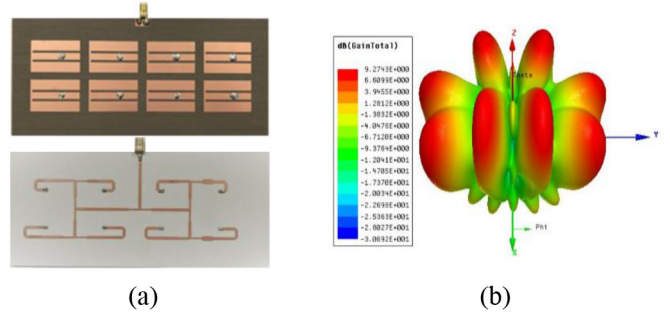


FIGURE 18. (a) 8-element multi-beam antenna array. (b) Radiation pattern with eight beams.

A printed dipole array with end-fire radiation is designed in terms of UMMPTTE in [25], which achieves the end-fire radiation through the ODE for all the array elements. In this way, neither reflectors nor directors are involved.

E. MULTI-BEAM ANTENNA ARRAYS [26], [27]

Multi-beam antennas simultaneously generate multiple beams and have found applications in satellite and mobile communications [119]–[122]. The WMMPTTE and CMMPTTE can be applied to the array design for multi-beam applications. By introducing multiple test Rx antennas in the directions where the beams are to be generated, the WMMPTTE and CMMPTTE produce the ODE to achieve multiple beams in the desired directions.

A four-element printed bidirectional dipole array is designed in terms of WMMPTTE in [26]. Compared with the conventional designs using dipole elements, the optimized dipole array can achieve a desired distribution of end-fire gains with reduced size and enhanced gain. The simulated and measured results show that the end-fire gain in one direction varies from 1.5 to 10.2 dBi at 2.45 GHz as the ratio of weights changes from 0 to 1. The end-fire gain reaches 9.3 dBi when the radiation pattern is equally shaped in both directions.

A four-element rectenna antenna array for RF power harvesting applications is presented in [27], in which the beamwidth of the array is enhanced by introducing two test Rx antennas in UMMPTTE so that two beams can be formed in the desired directions. It is shown that the enhanced beamwidth increases the output DC power significantly in comparison with the same antenna array fed by the uniform distribution of excitation.

A low-profile multi-beam antenna array consisting of eight E-shaped patch elements has been designed with WMMPTTE, whose configuration, the feeding circuit and radiation patterns are shown in Fig. 18. The antenna array operates at 5.8GHz and can generate eight squint beams in different directions simultaneously with a simple feeding circuit. The peak gains of the beams vary from 8.2 to 8.9 dBi. The multi-beam antenna array can be used as an indoor wireless base station installed on the ceiling or wall. In comparison with the similar applications in [123], the feeding network

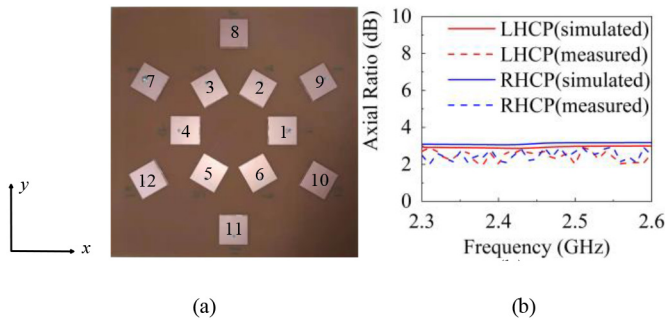


FIGURE 19. (a) 12-element polarization reconfigurable array. (b) Axial ratio.

obtained from MMPTE is much simpler, and the highest gain for each beam is guaranteed.

F. POLARIZATION-RECONFIGURABLE ANTENNA ARRAYS

The polarization-reconfigurable antenna arrays are usually realized by diodes, switches, and multi-ports feeding networks through controlling the operating modes of antenna elements [124], [125]. The MMPTE can also be applied to design of polarization-reconfigurable antennas. The array under design and a test receiving antenna form a wireless power transmission (WPT) system. The PTE is increased if the Tx and Rx antennas are polarization matched. For this reason, the polarization and the beam direction of the array under design can be simultaneously controlled by the polarization state and the position of the test receiving antenna through imposing that the PTE is maximized. The test receiving antenna can be chosen as a linearly polarized, a circularly polarized or a dual linearly polarized antenna placed in the desired beam direction, depending on the polarization to be achieved. As long as the array has the physical potential of realizing a designated polarization state, the MMPTE always produces an ODE for the array to realize the designated polarization state in the desired direction.

Fig. 19(a) shows a polarization-reconfigurable array working at 2.45GHz, which consists of 12 identical linearly polarized patch elements. The patch elements are purposely arranged so that the radiated electric field from the array has both x and y components. As a result, the array has the potential to realize multiple polarization states, such as x or y -polarized, dual linearly polarized, and circularly polarized, and the ODEs for achieving the polarization states can be obtained from UMMPTTE by introducing a test receiving antenna with desired polarization state. Fig. 19(b) gives the simulated and measured axial ratios for left-hand circular polarization (LHCP) state and right-hand circular polarization (RHCP) state.

Compared with other existing design methods, the polarization-reconfigurable antenna array designed by MMPTE has the advantages of high gain and low side lobes for a fixed array configuration as guaranteed by the MMPTE.

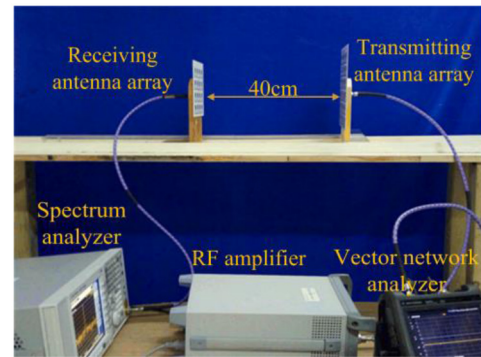


FIGURE 20. Measurement setup of WPT system.

V. OPTIMAL DESIGN OF WPT SYSTEMS

A WPT system generally consists of a transmitting array and a receiving array, and the power transmission efficiency naturally becomes the performance index for the design of antenna arrays. Much progress on the design of WPT systems has been made in recent decades [126]–[144], with the solar power satellite being considered the highest-potential application of WPT technology [126]–[131]. WPT technology has gradually been applied to other fields, such as wireless power distribution system in buildings, microwave hyperthermia, implantable devices and the vehicles powered by microwaves [132]. Various methods have been tried to improve the performances, efficiency, and robustness of WPT systems by dealing with the design of Tx arrays [133]–[142]. Moreover the power reaction factor can also be used as a performance index to design a WPT system [143], [144].

The application of MMPTE to the design of WPT system is straightforward. The PTE is a key performance index for the design of WPT system, and the MMPTE maximizes the PTE and therefore provides the best possible system performance. There are three application scenarios for the WPT systems, respectively corresponding to UMMPTTE, WMMPTE, and CMMPTTE.

A. DESIGN OF WPT SYSTEMS BY UMMPTTE [28]–[31]

The UMMPTTE corresponds to the scenario where no constraint is involved in the design of a WPT system. Two WPT systems operating at 5.8 GHz in free space are designed in terms of UMMPTTE in [29]. The first system is shown in Fig. 20 and uses a 36-element patch array as the Tx and a 16-element patch array as the Rx, separated by a distance of 40 cm so that the Tx and Rx arrays are in the Fresnel region of each other. The inset-fed patch is used as the array element. The feeding networks for both Tx and Rx arrays are designed according to the theory of transmission lines in terms of ODEs determined from (8) and (9) respectively. The antenna elements and the feeding network are printed on the same side of a 1.524 mm thick Rogers 4003 substrate with a relative dielectric constant of 3.55 and loss tangent of 0.0027. The measured PTE of the WPT system is 39.4%,

which is significantly higher than a similar design in [139] in view of the fact that the element number of the Tx array in the design with UMMPTE is only half of that used in [139]. The second system uses two identical 64-element arrays as the Tx and the Rx. The measured PTE reaches 46.9% when the two arrays are separated by a distance of 100 cm.

A WPT system operating at 1.9GHz for powering an implantable device, which is embedded in a human head model with relative dielectric constant of 39.9 and conductivity of 1.42 S/m and located in the radiative near field of the Tx array, is presented in [30]. The system is optimized by UMMPTE. Compared to a reference WPT system with the Tx array fed by the uniform amplitude and phase, the PTE of the optimized system is about 1.3 times that of the reference one.

The MMPTE can also be applied to the design of WPT system in an unknown electromagnetic environment [31]. Whenever the environment is unknown or too complicated to be modeled by a computer, the scattering parameters of the WPT system can be acquired by measurement, and the MMPTE is still applicable. The maximum PTE can be reached and the array can be optimized without identifying the electrical properties of the unknown environment.

B. DESIGN OF WPT SYSTEMS BY WMMPTE AND CMMPTE

Both WMMPTE and CMMPTE can be applied to achieve a specified distribution of received power among the Rx array elements. The WMMPTE is most suitable for the situation where the power levels are required to be different among the Rx array elements (e.g., different electronic devices are simultaneously powered). The CMMPTE is most applicable to the scenario where the distribution of received power must be flat along the Rx array elements (e.g., several closely spaced identical electronic devices are wirelessly powered). The UMMPTE, WMMPTE and CMMPTE have been applied to the design of a same WPT system operating at 2.45GHz, in which the Tx array consists of 36 square patch elements and arranged as a square; and the Rx array consists of 5 square patch elements arranged as an L shape. The Tx and Rx arrays are separated by a distance of 15cm. Fig. 21 shows the simulation model for the WPT system.

The Tx and Rx arrays are built on a 3mm-thick FR4 substrate. The three formulations of MMPTE yield three feeding schemes for both Tx and Rx arrays, corresponding to three different application scenarios. Simulation and experiment indicate that the PTEs corresponding to UMMPTE, WMMPTE and CMMPTE are 22.4%, 15.1% and 11.4% respectively. The highest PTE is given by UMMPTE since it does not involve any constraints. The CMMPTE yields the lowest PTE as it requires that the received energy is equally distributed along the whole path of the L-shape while the WMMPTE only requires that the radiated energy is equally distributed at the locations where the Rx elements are placed.

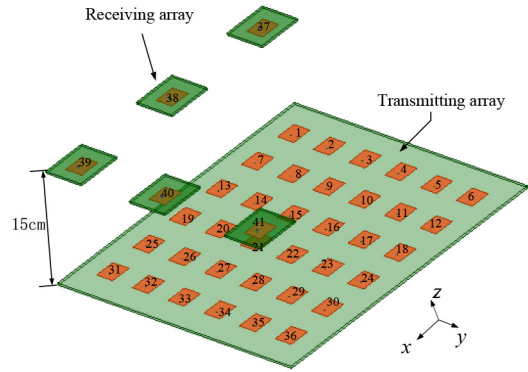


FIGURE 21. Simulation model for WPT system.

VI. CONCLUSION

In summary, one can make use of the PTE as an objective function to be maximized to design various WPT systems, and such an optimization design technique is referred to as MMPTE. By introducing a test Rx array, the optimal design of an antenna array can be converted to the optimal design of a WPT system. The ODE obtained from MMPTE for the antenna array guarantees that the gain of the array is maximized for a fixed array configuration. There are three different formulations of MMPTE, respectively referred to as UMMPTE, WMMPTE and CMMPTE, and they can be extended to different versions by replacing the test receiving antennas with selected volumes or surfaces. The PTE for the extended MMPTE is defined by the ratio of the weighted sum of the radiated energies in the volumes or the radiated power through the surfaces over the total input power into the Tx antenna array.

The MMPTE exhibits some remarkable features:

- 1) It breaks through the limitations that lie in the conventional array design methods when the pattern multiplication rule fails, and is applicable to the design of antenna array of any type or configuration.
- 2) The MMPTE reduces the field synthesis problem into a circuit analysis problem, and is thus easy to master and implement, and is more accessible for those who are not very familiar with the EM field theory.
- 3) The MMPTE can incorporate the information about the environments around the Tx and Rx arrays, and therefore it can be made adaptive to any complicated environment.
- 4) The MMPTE always provides an optimal solution to the array design problem wherever such a solution physically exists for a fixed configuration of the array.

Like the other array design methods, the computational time of the MMPTE grows as the size of the array increases. Whenever the computational resources are not available, or the system is too complicated to be handled with a state-of-the-art computer, one can make use of measurement to determine the scattering parameters in the MMPTE formulation.

One of the important issues that has not been discussed in this article is the design of wideband antenna array. In order to determine the ODEs across the wide frequency band, one can select multiple frequency points in the band and follow the single-frequency formulation to find the ODE for each frequency point. To realize the ODEs at multiple frequency points, it is inevitable to increase the complexity of the feeding networks, which is an issue to be solved in the future.

REFERENCES

- [1] R. C. Hanson, *Phased Antenna Arrays*. Hoboken, NJ, USA: Wiley, 1998.
- [2] L. Titarenko and A. Barkalov, *Methods of Signal Processing for Adaptive Antenna Arrays*. Heidelberg, Germany: Springer, 2013.
- [3] R. Cicchetti, A. Faraone, and O. Testa, "Energy-based representation of multipoint circuits and antennas suitable for near- and far-field syntheses," *IEEE Trans. Antennas Propag.*, vol. 67, no. 1, pp. 85–98, Jan. 2019.
- [4] W. Geyi, *Foundations of Applied Electrodynamics*. New York, NY, USA: Wiley, 2010, ch. 6.
- [5] W. Geyi, *Foundations for Radio Frequency Engineering*. London, U.K.: World Sci., 2015, ch. 5.
- [6] W. Geyi, "Optimal design of antenna arrays (Invited)," in *Proc. IEEE Int. Workshop Antenna Technol.*, Sydney, NSW, Australia, Mar. 2014, doi: [10.1109/IWAT.2014.6958621](https://doi.org/10.1109/IWAT.2014.6958621).
- [7] W. Geyi, "A universal method for the design of antenna arrays (invited)," in *Proc. Progr. Electromagn. Res. (PIER)*, Prague, Czech, Jul. 2015.
- [8] W. Geyi and Y. Jiang, "Optimum design of a printed 2.45 Ghz end-fire dipole array(invited)," in *Proc. IEEE Conf. Antenna Meas. Appl. (IEEE CAMA)*, Chiangmai, Thailand, Nov./Dec. 2015, doi: [10.1109/CAMA.2015.7428172](https://doi.org/10.1109/CAMA.2015.7428172).
- [9] W. Geyi and S. Hucheng, "Controlling electromagnetic fields in complex environments(invited)," in *Proc. IEEE Asia-Pac. Conf. Antennas Propag. (APCAP)*, Auckland, New Zealand, Aug. 2018, doi: [10.1109/APCAP.2018.8538305](https://doi.org/10.1109/APCAP.2018.8538305).
- [10] W. Geyi, "A universal method for field controls: Invited," in *Proc. URSI Int. Symp. Electromagn. Theory (EMTS)*, San Diego, CA, USA, May 2019.
- [11] L. Shan and W. Geyi, "Optimal design of focused antenna arrays," *IEEE Trans. Antennas Propag.*, vol. 62, no. 11, pp. 5565–5571, Nov. 2014.
- [12] X. Y. Wang, G. M. Yang, and W. Geyi, "A new design of focused antenna arrays," *Microw. Opt. Techn. Lett.*, vol. 56, no. 10, pp. 2464–2468, Oct. 2014.
- [13] Y. H. Jiang, W. Geyi, L. S. Yang, and H. Sun, "Circularly-polarized focused microstrip antenna arrays," *IEEE Antennas Wireless Propag. Lett.*, vol. 15, pp. 52–57, 2016.
- [14] Y. H. Jiang, W. Geyi, and H. Sun, "A new focused antenna array with circular polarization," *Microw. Opt. Techn. Lett.*, vol. 57, no. 12, pp. 2936–2939, Dec. 2015.
- [15] X. P. He, W. Geyi, and S. Y. Wang, "Optimal design of focused arrays for microwave-induced hyperthermia," *IET Microw. Antennas Propag.*, vol. 9, no. 14, pp. 1605–1611, 2015.
- [16] X. P. He, W. Geyi, and S. Y. Wang, "A hexagonal focused array for microwave hyperthermia: Optimal design and experiment," *IEEE Antennas Wireless Propag. Lett.*, vol. 15, pp. 1605–1611, 2016.
- [17] X. Cai, X. Gu, and W. Geyi, "Optimal design of antenna arrays focused on multiple targets," *IEEE Trans. Antennas Propag.*, vol. 68, no. 6, pp. 4593–4603, Jun. 2020, doi: [10.1109/TAP.2020.2972311](https://doi.org/10.1109/TAP.2020.2972311).
- [18] T. Li and W. Geyi, "Design of MIMO beamforming antenna array for mobile handsets," *Progr. Electromagn. Res. C*, vol. 94, pp. 13–28, Jul. 2019.
- [19] H. Tong and W. Geyi, "Optimal design of smart antenna systems for handheld devices," *IET Microw. Antennas Propag.*, vol. 10, no. 6, pp. 617–623, 2016.
- [20] W. Wan, W. Geyi, and S. Gao, "Optimum design of low-cost dual-mode beam-steerable arrays for customer-premises equipment applications," *IEEE Access*, vol. 6, pp. 16092–16098, 2018.
- [21] X. Miao, W. Wan, Z. Duan, and W. Geyi, "Design of dual-mode arc-shaped dipole arrays for indoor base-station applications," *IEEE Antennas Wireless Propag. Lett.*, vol. 18, no. 4, pp. 752–756, Apr. 2019.
- [22] X. Cai and W. Geyi, "An optimization method for the synthesis of flat-top radiation patterns in the near- and far-field regions," *IEEE Trans. Antennas Propag.*, vol. 67, no. 2, pp. 980–987, Feb. 2019.
- [23] X. Gu and W. Geyi, "Design of a near-field RFID antenna array in metal cabinet environment," *IEEE Antennas Wireless Propag. Lett.*, vol. 18, no. 1, pp. 79–83, Jan. 2019.
- [24] H. Guo and W. Geyi, "Design of Yagi-Uda antenna with multiple driven elements," *Progr. Electromagn. Res. C*, vol. 92, pp. 101–112, Apr. 2019.
- [25] X. Cai, W. Geyi, and H. C. Sun, "A printed dipole array with high gain and end-fire radiation," *IEEE Antennas Wireless Propag. Lett.*, vol. 16, pp. 1512–1515, 2017.
- [26] H. Guo and W. Geyi, "Design of bidirectional antenna array with adjustable endfire gains," *IEEE Antennas Wireless Propag. Lett.*, vol. 18, no. 8, pp. 1656–1660, Aug. 2019.
- [27] H. C. Sun and W. Geyi, "A new rectenna using beamwidth-enhanced antenna array for RF power harvesting applications," *IEEE Antennas Wireless Propag. Lett.*, vol. 16, pp. 1451–1454, 2017.
- [28] F. Xie, G. Yang, and W. Geyi, "Optimal design of an antenna array for energy harvesting," *IEEE Antennas Wireless Propag. Lett.*, vol. 12, pp. 155–158, 2013.
- [29] X. D. Yang, W. Geyi, and H. C. Sun, "Optimum design of wireless power transmission system using microstrip patch antenna arrays," *IEEE Antennas Wireless Propag. Lett.*, vol. 16, pp. 1824–1827, 2017.
- [30] Z. Z. Chen, H. C. Sun, and W. Geyi, "Wireless powering system for the implantable device in the radiative near-field," *IEEE Antennas Wireless Propag. Lett.*, vol. 16, pp. 1780–1783, 2017.
- [31] H. C. Sun and W. Geyi, "Optimum design of wireless power transmission systems in unknown electromagnetic environments," *IEEE Access*, vol. 5, pp. 20198–20206, 2017.
- [32] M. K. Hu, "Near zone power transmission formulae," in *IRE National Convention Record*. New York, NY, USA: Inst. Radio Eng., 1958, pp. 128–135.
- [33] G. Goubao and F. Schwinger, "On the guided propagation of electromagnetic wave beams," *IRE Trans. Antennas Propag.*, vol. 9, no. 3, pp. 248–256, May 1961.
- [34] A. F. Key, "Near field gain of aperture antennas," *IRE Trans. Antennas Propag.*, vol. 8, no. 6, pp. 586–593, Nov. 1961.
- [35] J. W. Sherman, "Properties of focused aperture in the Fresnel region," *IRE Trans. Antennas Propag.*, vol. 10, no. 4, pp. 399–408, Jul. 1962.
- [36] W. J. Graham, "Analysis and synthesis of axial field patterns of focused apertures," *IEEE Trans. Antennas Propag.*, vol. AP-31, no. 4, pp. 665–668, Jul. 1983.
- [37] G. V. Borgiotti, "Maximum power transfer between two planner aperture in the Fresnel zone," *IEEE Trans. Antennas Propag.*, vol. AP-14, no. 2, pp. 158–163, Mar. 1966.
- [38] E. C. Okress, *Microwave Power Engineering*, vols. 1–2. New York, NY, USA: Academic, 1968.
- [39] W. Geyi, "Theoretical study for microwave power transmission," *J. Electron.*, vol. 20, no. 4, pp. 538–545, Jul. 1998.
- [40] R. A. Horn and C. R. Johnson, *Matrix Analysis*. Cambridge, U.K.: Cambridge Univ. Press, 2013.
- [41] J. R. Bar-On and K. A. Grasse, "Global optimization of a quadratic functional with quadratic equality constraints, part 2," *J. Optim. Theory Appl.*, vol. 93, no. 3, pp. 547–556, Aug. 1997.
- [42] Z. H. Jia, X. J. Cai, and D. R. Han, "Comparison of several fast algorithms for projection onto an ellipsoid," *J. Comput. Appl. Math.*, vol. 319, pp. 320–337, Aug. 2017.
- [43] H. Lang and C. D. Sattis, "Optimization of wireless power transfer systems enhanced by passive elements and metasurfaces," *IEEE Trans. Antennas Propag.*, vol. 65, no. 10, pp. 5462–5474, Oct. 2017.
- [44] M. Böhm and A. Louis, "Efficient algorithm for computing optimal control of antennas in hyperthermia," *Survey Math. Ind.*, vol. 3, no. 4, pp. 233–251, 1993.
- [45] T. Köhler, P. Maass, P. Wust, and M. Seebass, "A fast algorithm to find optimal controls of multiantenna applicators in regional hyperthermia," *Phys. Med. Biol.*, vol. 46, no. 9, pp. 2503–2514, 2010.

- [46] M. Bogosanic and A. G. Williamson, "Microstrip antenna array with a beam focused in the near-field zone for application in noncontact microwave industrial inspection," *IEEE Trans. Instrum. Meas.*, vol. 56, no. 6, pp. 2186–2195, Dec. 2007.
- [47] K. D. Stephan, J. B. Mead, D. M. Pozar, L. Wang, and J. A. Pearce, "A near field focused microstrip array for a radiometric temperature sensor," *IEEE Trans. Antennas Propag.*, vol. 55, no. 4, pp. 1199–1203, Apr. 2007.
- [48] W. Gee, S. W. Lee, N. K. Bong, C. A. Cain, R. Mittra, and R. L. Magin, "Focused array hyperthermia applicator: Theory and experiment," *IEEE Trans. Biomed. Eng.*, vol. BME-31, no. 1, pp. 38–46, Jan. 1984.
- [49] J. T. Loane and S. Lee, "Gain optimization of a near-field focusing array for hyperthermia application," *IEEE Trans. Microw. Theory Tech.*, vol. 37, no. 10, pp. 1629–1635, Oct. 1989.
- [50] C. J. Diederich and K. Hynynen, "The feasibility of using electrically focused ultrasound arrays to induce deep hyperthermia via body cavities," *IEEE Trans. Ultrason., Ferroelect., Freq. Control*, vol. 38, no. 3, pp. 207–218, May 1991.
- [51] F. Tofigh, J. Nourinia, M. Azarmanesh, and K. M. Khazaei, "Near-field focused array microstrip planar antenna for medical applications," *IEEE Antennas Wireless Propag. Lett.*, vol. 13, pp. 915–954, 2014.
- [52] R. Siragusa, P. Lemaitre-Auger, and S. Tedjini, "Near field focusing circular microstrip antenna array for RFID applications," in *IEEE Int. Symp. Antennas Propag. Dig.*, Jun. 2009, pp. 1–4.
- [53] D. Paret, *Antenna Designs for NFC Devices*. Hoboken, NJ, USA: Wiley, 2016.
- [54] C. H. Weng, C. F. Yang, Y. S. Lin, F. S. Chen, Y. C. Huang, and C. W. Hsu, "Design of RFID near-field focusing circular patch array antenna at 2.4 GHz with applications," in *Proc. Internet Things (IOT)*, Dec. 2010, pp. 1–4.
- [55] A. Buffi, A. A. Serra, P. Nepa, H. T. Chou, and G. Manara, "A focused planar microstrip array for 2.4 GHz RFID readers," *IEEE Trans. Antennas Propag.*, vol. 58, no. 5, pp. 1536–1544, Mar. 2010.
- [56] P. Nepa and A. Buffi, "Near-field-focused microwave antennas: Near-field shaping and implementation," *IEEE Antennas Propag. Mag.*, vol. 59, no. 3, pp. 42–53, Jun. 2017.
- [57] P. Nepa, A. Buffi, A. Michel, and G. Manara, "Technologies for near-field focused microwave antennas," *Int. J. Antennas Propag.*, vol. 2017, pp. 1–17, Jun. 2017.
- [58] S. Karimkashi and A. A. Kishk, "Focused microstrip array antenna using a Dolph–Chebyshev near-field design," *IEEE Trans. Antennas Propag.*, vol. 57, no. 12, pp. 3813–3820, Dec. 2009.
- [59] G. Lerosey, J. de Rosny, A. Tourin, A. Derode, G. Montaldo, and M. Fink, "Time reversal of electromagnetic waves," *Phys. Rev. Lett.*, vol. 92, no. 19, 2004, Art. no. 193904.
- [60] D. Zhao and M. Zhu, "Generating microwave spatial fields with arbitrary patterns," *IEEE Antennas Wireless Propag. Lett.*, vol. 15, pp. 1739–1742, 2016.
- [61] D. Zhao, Y. Jin, B.-Z. Wang, and R. Zang, "Time reversal based broadband synthesis method for arbitrarily structured beam-steering arrays," *IEEE Trans. Antennas Propag.*, vol. 60, no. 1, pp. 164–173, Jan. 2012.
- [62] M. Fink, "Time reversed acoustics," *Phys. Today*, vol. 50, pp. 34–40, Mar. 1997.
- [63] M. Soma, D. C. Galbraith, and R. L. White, "Radio-frequency coils in implantable devices: Misalignment analysis and design procedure," *IEEE Trans. Biomed. Eng.*, vol. BME-34, no. 4, pp. 276–282, Apr. 1987.
- [64] P. R. Troyk and M. A. K. Schwan, "Closed-loop class E transcutaneous power and data link for microimplants," *IEEE Trans. Biomed. Eng.*, vol. 39, no. 6, pp. 589–599, Jun. 1992.
- [65] E. Y. Chow, C.-L. Yang, Y. Ouyang, A. L. Chlebowski, P. P. Irazoqui, and W. J. Chappell, "Wireless powering and the study of RF propagation through ocular tissue for development of implantable sensors," *IEEE Trans. Antennas Propag.*, vol. 59, no. 6, pp. 2379–2387, Jun. 2011.
- [66] J. Alvarez, R. G. Ayestaran, and F. Las-Heras, "Design of antenna arrays for near-field focusing requirements using optimization," *Electron. Lett.*, vol. 48, no. 21, pp. 1323–1325, Oct. 2012.
- [67] J. Alvarez *et al.*, "Near field multifocusing on antenna arrays via non-convex optimization," *IET Microw. Antennas Propag.*, vol. 8, no. 10, pp. 754–764, Jul. 2014.
- [68] R. G. Ayestaran, "Fast near-field multifocusing of antenna arrays including element coupling using neural networks," *IEEE Antennas Wireless Propag. Lett.*, vol. 17, no. 7, pp. 1233–1237, Jul. 2018.
- [69] A. Ungureanu, Y. Fu, T. P. Vuong, and F. Ndagijimana, "Electromagnetic source synthesis by reversed-TLM method," in *IEEE MTT-S Int. Microw. Symp. Dig.*, Baltimore, MD, USA, Jun. 2011, pp. 373–376.
- [70] M. Donelli, I. Craddock, D. Gibbins, and M. Sarafianou, "Modelling complex electromagnetics sources for microwave imaging systems with wave field synthesis technique," *Electron. Lett.*, vol. 48, no. 23, pp. 1478–1479, Nov. 2012.
- [71] P. P. M. So and W. J. R. Hofer, "Source reconstruction with super-resolution using TLM time reversal," in *IEEE MTT-S Int. Microw. Symp. Dig.*, Tampa Bay, FL, USA, Jun. 2014, pp. 1–4.
- [72] D. S. Zhao, "Shaping microwave field of arbitrary intensity patterns in bounded area by time reversal mirror," in *Proc. PIERS*, Shanghai, China, Aug. 2016, doi: [10.1109/PIERS.2016.7735642](https://doi.org/10.1109/PIERS.2016.7735642).
- [73] J. W. Wu, R. Y. Wu, X. C. Bao, L. Bao, X. J. Fu, and T. J. Cui, "Synthesis algorithm for near-field power pattern control and its experimental verification via metasurfaces," *IEEE Trans. Antennas Propag.*, vol. 67, no. 2, pp. 1073–1083, Feb. 2019.
- [74] M. I. Skolnik, *Introduction to Radar Systems*. New York, NY, USA: McGraw-Hill, 1980.
- [75] S. Haykin and A. Steinhardt, Eds. *Adaptive Radar Detection and Estimation*. New York, NY, USA: Wiley, 1992.
- [76] M. Chryssomallis, "Smart antennas," *IEEE Antennas Propag. Mag.*, vol. 42, no. 3, pp. 129–136, May 2000.
- [77] C. Sun, J. Cheng, and T. Ohira, *Handbook on Advancements in Smart Antenna Technologies for Wireless Networks*. New York, NY, USA: Inf. Sci., 2009.
- [78] M.-I. Lai, T.-Y. Wu, J.-C. Hsieh, C.-H. Wang, and S.-K. Jeng, "Compact switched-beam antenna employing a four-element slot antenna array for digital home applications," *IEEE Trans. Antennas Propag.*, vol. 56, no. 9, pp. 2929–2936, Sep. 2008.
- [79] Z. J. Chen and C. Parini, "Low cost shaped beam synthesis for semi-smart base station antennas," *IET Microw. Antennas Propag.*, vol. 10, pp. 119–128, Apr. 2015.
- [80] M. Ibrahim, M. Elamin, and T. A. Rahman, "2-element slot meander patch antenna system for LTE-WLAN customer premise equipment," in *Proc. IEEE-APS Topical Conf. Antennas Propag. Wireless Commun. (APWC)*, 2015, pp. 993–996.
- [81] P. M. Woodward and J. D. Lawson, "The theoretical precision with which an arbitrary radiation-pattern may be obtained from a source of finite size," *J. Inst. Elect. Eng. III Radio Commun. Eng.*, vol. 95, no. 37, pp. 515–518, Oct. 1948.
- [82] S. A. Schelkunoff, "A mathematical theory of linear arrays," *Bell Syst. Tech. Freq.*, vol. 22, no. 1, pp. 80–107, Jan. 1943.
- [83] A. Chakraborty, B. N. Das, and G. S. Sanyal, "Beam shaping using nonlinear phase distribution in a uniformly spaced array," *IEEE Trans. Antennas Propag.*, vol. AP-30, no. 5, pp. 1031–1034, Sep. 1982.
- [84] R. S. Elliott and G. J. Stern, "A new technique for shaped beam synthesis of equispaced arrays," *IEEE Trans. Antennas Propag.*, vol. AP-32, no. 10, pp. 515–518, Oct. 1984.
- [85] H. J. Orchard, R. S. Elliott, and G. J. Stern, "Optimising the synthesis of shaped beam antenna patterns," *IEE Proc. H Microw. Antennas Propag.*, vol. 132, no. 1, pp. 63–68, 1985.
- [86] W. Stutzman, "Synthesis of shaped-beam radiation patterns using the iterative sampling method," *IEEE Trans. Antennas Propag.*, vol. AP-19, no. 1, pp. 36–41, Jan. 1971.
- [87] F. J. Ares-Pena, J. A. Rodriguez-Gonzalez, E. Villanueva-Lopez, and S. R. Rengarajan, "Genetic algorithms in the design and optimization of antenna array patterns," *IEEE Trans. Antennas Propag.*, vol. 47, no. 3, pp. 506–510, Mar. 1999.
- [88] T. Su and H. Ling, "Array beamforming in the presence of a mounting tower using genetic algorithms," *IEEE Trans. Antennas Propag.*, vol. 53, no. 6, pp. 2011–2019, Jun. 2005.
- [89] F. J. Villegas, "Parallel genetic-algorithm optimization of shaped beam coverage areas using planar 2-D phased arrays," *IEEE Trans. Antennas Propag.*, vol. 55, no. 6, pp. 1745–1753, Jun. 2007.
- [90] F. Ares, S. Rengarajan, E. Villanueva, E. Skochinski, and E. Moreno, "Application of genetic algorithms and simulated annealing technique in optimising the aperture distributions of antenna array patterns," *Electron. Lett.*, vol. 32, no. 3, pp. 148–149, Feb. 1996.

- [91] J. A. Ferreira and F. Ares, "Pattern synthesis of conformal arrays by the simulated annealing technique," *Electron. Lett.*, vol. 33, no. 14, pp. 1187–1189, Jul. 1997.
- [92] D. W. Boeringer and D. H. Werner, "Particle swarm optimization versus genetic algorithms for phased array synthesis," *IEEE Trans. Antennas Propag.*, vol. 52, no. 3, pp. 771–779, Mar. 2004.
- [93] D. W. Boeringer and D. H. Werner, "Efficiency-constrained particle swarm optimization of a modified bernstein polynomial for conformal array excitation amplitude synthesis," *IEEE Trans. Antennas Propag.*, vol. 53, no. 8, pp. 2662–2673, Aug. 2005.
- [94] J. Y. Li, Y. X. Qi, and S. G. Zhou, "Shaped beam synthesis based on superposition principle and Taylor method," *IEEE Trans. Antennas Propag.*, vol. 65, no. 11, pp. 6157–6160, Nov. 2017.
- [95] A. Akdagli and K. Guney, "Shaped-beam pattern synthesis of equally and unequally spaced linear antenna arrays using a modified tabu search algorithm," *Microw. Opt. Technol. Lett.*, vol. 36, no. 1, pp. 16–20, Jan. 2003.
- [96] C. Lin, A. Qing, and Q. Feng, "Synthesis of unequally spaced antenna arrays by using differential evolution," *IEEE Trans. Antennas Propag.*, vol. 58, no. 8, pp. 2553–2561, Aug. 2010.
- [97] H. Wang, Z. J. Zhang, and Z. H. Feng, "A beam-switching antenna array with shaped radiation patterns" *IEEE Antennas Wireless Propag. Lett.*, vol. 11, pp. 818–821, Nov. 2012.
- [98] A. Ksienski, "Maximally flat and quasi-smooth sector beams," *IRE Trans. Antennas Propag.*, vol. 8, no. 5, pp. 476–484, Sep. 1960.
- [99] O. M. Bucci, G. D'elia, G. Mazzarella, and G. Panariello, "Antenna pattern synthesis: A new general approach," *Proc. IEEE*, vol. 82, no. 3, pp. 359–371, Mar. 1994.
- [100] R. S. Elliot, *Antenna Theory and Design*. Englewood Cliffs, NJ, USA: Prentice-Hall, 1981.
- [101] C. A. Balanis, *Antenna Theory: Analysis and Design*. New York, NY, USA: Wiley, 1997.
- [102] D. Gies and Y. Rahmat-Samii, "Particle swarm optimization for reconfigurable phase-differentiated array design," *Microwave Opt. Technol. Lett.*, vol. 38, no. 3, pp. 172–175, Aug. 2003.
- [103] J. M. Johnson and Y. Rahmat-Samii, "Genetic algorithms in engineering electromagnetics," *IEEE Trans. Antennas Propag.*, vol. 39, no. 4, pp. 7–25, Aug. 1997.
- [104] R. J. Allard, D. H. Werner, and P. L. Werner, "Radiation pattern synthesis for arrays of conformal antennas mounted on arbitrarily-shaped three-dimensional platforms using generic algorithms," *IEEE Trans. Antennas Propag.*, vol. 51, no. 5, pp. 1054–1062, May 2003.
- [105] D. A. Hill, "A numerical method for near-field array synthesis," *IEEE Trans. Electromagn. Comp.*, vol. EMC-27, no. 4, pp. 201–211, Nov. 1985.
- [106] B. Stupfel and S. Vermersch, "Plane-wave synthesis by an antenna-array and RCS determination: Theoretical approach and numerical simulations," *IEEE Trans. Antennas Propag.*, vol. 52, no. 11, pp. 3086–3095, Nov. 2004.
- [107] M. S. Narasimhan and B. Philips, "Synthesis of near-field patterns of arrays," *IEEE Trans. Antennas Propag.*, vol. AP-35, no. 2, pp. 212–218, Feb. 1987.
- [108] H. T. Chou, N. N. Wang, H. H. Chou, and J. H. Qiu, "An effective synthesis of planar array antennas for producing near-field contoured patterns," *IEEE Trans. Antennas Propag.*, vol. 59, no. 9, pp. 3224–3233, Sep. 2011.
- [109] Z. X. Huang and Y. J. Cheng, "Near-field pattern synthesis for sparse focusing antenna arrays based on Bayesian Compressive Sensing and convex optimization," *IEEE Trans. Antennas Propag.*, vol. 66, no. 10, pp. 5249–5257, Oct. 2018.
- [110] S. Uda, "Wireless beam of short electric waves," *J. Inst. Elect. Eng.*, vol. 452, pp. 273–282, Mar. 1926.
- [111] H. Yagi, "Beam transmission of the ultra short waves," *Proc. IRE*, vol. 16, pp. 715–741, Jun. 1928.
- [112] J. Huang and A. Densmore, "Microstrip Yagi antenna for mobile satellite vehicle application," *IEEE Trans. Antennas Propag.*, vol. 39, no. 7, pp. 1024–1030, Jul. 1991.
- [113] G. R. DeJean and M. M. Tentzeris, "A new high-gain microstrip Yagi array antenna with a high front-to-back (F/B) ratio for WLAN and millimeter-wave applications," *IEEE Trans. Antennas Propag.*, vol. 55, no. 2, pp. 298–304, Feb. 2007.
- [114] W. R. Deal, N. Kaneda, J. Sor, Y. Qian, and T. Itoh, "A new quasi-Yagi antenna for planar active antenna arrays," *IEEE Trans. Microw. Theory Techn.*, vol. 48, no. 6, pp. 910–918, Jun. 2000.
- [115] P. R. Grajek, B. Schoenlinner, and G. M. Rebeiz, "A 24 GHz high-gain Yagi-Uda antenna array," *IEEE Trans. Antennas Propag.*, vol. 52, no. 5, pp. 1257–1261, May 2004.
- [116] D. Gray, J. Lu, and D. Thiel, "Electronically steerable Yagi-Uda microstrip patch antenna array," *IEEE Trans. Antennas Propag.*, vol. 46, no. 5, pp. 605–608, May 1998.
- [117] J. Liu and Q. Xue, "Microstrip magnetic dipole Yagi array antenna with endfire radiation and vertical polarization," *IEEE Trans. Antennas Propag.*, vol. 61, no. 3, pp. 1140–1147, Mar. 2013.
- [118] P. Aguilà, S. Zuffanelli, G. Zamora, F. Paredes, F. Martín, and J. Bonache, "Planar Yagi-Uda antenna array based on split-ring resonators (SRRs)," *IEEE Antennas Wireless Propag. Lett.*, vol. 16, pp. 1233–1236, May 2017.
- [119] J. Allen, "A theoretical limitation on the formation of lossless multiple beams in linear arrays," *IRE Trans. Antennas Propag.*, vol. 9, no. 4, pp. 350–352, Jul. 1961.
- [120] R. Jorgensen, P. Balling, and W. English, "Dual offset reflector multibeam antenna for international communications satellite applications," *IEEE Trans. Antennas Propag.*, vol. AP-33, no. 12, pp. 1304–1312, Dec. 1985.
- [121] A. I. Zaghloul, Y. Hwang, R. M. Sorbello, and F. T. Assal, "Advances in multibeam communications satellite antennas," *Proc. IEEE*, vol. 78, no. 7, pp. 1214–1232, Jul. 1990.
- [122] W. Hong *et al.*, "Multibeam antenna technologies for 5G wireless communications," *IEEE Trans. Antennas Propag.*, vol. 65, no. 12, pp. 6231–6249, Dec. 2017.
- [123] J. F. Keh, M. Chou, Z. C. Zhang, Q. X. An, and W. J. Liao, "A beam forming network based four-squint-beam array antenna for ceiling-mount access point," *IEEE Antennas Wireless Propag. Lett.*, vol. 18, no. 4, pp. 707–711, Apr. 2019.
- [124] N. Zhu, X. Yang, T. Lou, Q. Cao, and S. Gao, "Broadband polarization-reconfigurable slot antenna and array with compact feed network," *IEEE Antennas Wireless Propag. Lett.*, vol. 18, no. 6, pp. 1293–1297, Jun. 2019.
- [125] K. Li, Y. Shi, H. Shen, and L. Li, "A characteristic-mode-based polarization-reconfigurable antenna and its array," *IEEE Access*, vol. 6, pp. 64587–64595, 2018.
- [126] W. C. Brown, "The history of power transmission by radio waves," *IEEE Trans. Microw. Theory Techn.*, vol. MIT-32, no. 9, pp. 1230–1242, Sep. 1984.
- [127] W. C. Brown and E. Eves, "Beamed microwave power transmission and its application to space," *IEEE Trans. Microw. Theory Techn.*, vol. 40, no. 6, pp. 1239–1250, Jun. 1992.
- [128] J. O. Mcspadden and J. C. Mankins, "Space solar power programs and microwave wireless power transmission technology," *IEEE Microw. Mag.*, vol. 3, no. 4, pp. 46–57, Dec. 2002.
- [129] N. Shinohara and H. Matsumoto, "Experimental study of large rectenna array for microwave energy transmission," *IEEE Trans. Microw. Theory Techn.*, vol. 46, no. 3, pp. 261–268, Mar. 1998.
- [130] H. Matsumoto, "Research on solar power station and microwave power transmission in Japan: Review and perspectives," *IEEE Microw. Mag.*, vol. 3, no. 4, pp. 36–45, Dec. 2002.
- [131] K. Tanaka, K. Maki, M. Takahashi, and S. Sasaki, "Microwave power transmission experiment using breadboard model for small scientific satellite toward SPS," in *Proc. Int. Conf. Electromagn. Adv. Appl.*, 2012, pp. 666–669.
- [132] N. Shinohara, *Wireless Power Transfer Via Radiowaves*. Hoboken, NJ, USA: Wiley, 2014.
- [133] Y. Li and V. Jandhyala, "Design of retrodirective antenna arrays for short-range wireless power transmission," *IEEE Trans. Antennas Propag.*, vol. 60, no. 1, pp. 206–211, Jan. 2012.
- [134] G. Franceschetti, A. Massa, and P. Rocca, "Innovative antenna systems for efficient microwave power collection," in *Proc. IEEE Int. Microw. Workshop Innov. Wireless Power Transm. Technol. Syst. Appl. (IMWS)*, May 2011, pp. 275–278.
- [135] T. Narita, T. Kimura, K. Anma, N. Fukuda, and N. Shinohara, "Development of high accuracy phase control method for space solar power system," in *Proc. IEEE Int. Microw. Workshop Series Innov. Wireless Power Transm. Techn. Syst.*, May 2011, pp. 227–230.
- [136] V. Jamnejad and A. Hoorfar, "Optimization of antenna beam transmission efficiency," in *Proc. IEEE Antennas Propag. Soc. Int. Symp.*, San Diego, CA, USA, Jul. 2008, pp. 1–4.

- [137] A. K. M. Baki, K. Hashimoto, N. Shinohara, T. Mitani, and H. Matsumoto, "New and improved method of beam forming with reduced side lobe levels for microwave power transmission," in *Proc. Int. Conf. Elect. Comput. Eng.*, Dhaka, Bangladesh, Dec. 2008, pp. 773–777.
- [138] G. Oliveri, P. Rocca, F. Viani, F. Robol, and A. Massa, "Latest advances and innovative solutions in antenna array synthesis for microwave wireless power transmission," in *Proc. IEEE Microw. Workshop Series Innov. Wireless Power Trans. Technol. Syst. Appl.*, 2012, pp. 71–73.
- [139] V. Gowda, O. Yurduseven, G. Lipworth, and T. Zupan, "Wireless power transfer in the radiative near-field," *IEEE Antennas Wireless Propag. Lett.*, vol. 15, pp. 1865–1868, 2016.
- [140] X. Li, K. M. Luk, and B. Duan, "Aperture illumination designs for microwave wireless power transmission with constraints on edge tapers using bezier curves," *IEEE Trans. Antennas Propag.*, vol. 67, no. 4, pp. 2739–2944, Feb. 2019.
- [141] X. Li, K. M. Luk, and B. Duan, "Multiobjective optimal antenna synthesis for microwave wireless power transmission," *IEEE Trans. Antennas Propag.*, vol. 67, no. 2, pp. 1380–1385, Apr. 2019.
- [142] X. Yi, X. Chen, L. Zhou, S. Hao, B. Zhang, and X. Duan, "A microwave power transmission experiment based on the near-field focused transmitter," *IEEE Trans. Antennas Propag.*, vol. 18, no. 6, pp. 1105–1108, Jun. 2019.
- [143] H.-T. Chou, "Maximization of mutual reaction between two conformal phased arrays of antennas to enhance power transfer in radiating near-field region," *IEEE J. Radio Freq. Identification*, vol. 4, no. 4, pp. 506–516, Dec. 2020.
- [144] H.-T. Chou, "Conformal near-field focus radiation from phased array of antennas to enhance power transfer between transmitting and receiving antennas," *IEEE Trans. Antennas Propag.*, vol. 68, no. 5, pp. 3567–3577, May 2020.



WEN GEYI (Fellow, IEEE) was born in Pingjiang, China, in 1963. He received the B.Eng., M.Eng., and Ph.D. degrees in electrical engineering from Xidian University, Xi'an, China, in 1982, 1984, and 1987, respectively. From 1988 to 1990, he was a Lecturer with the Radio Engineering Department, Southeast University, Nanjing, China. From 1990 to 1992, he was an Associate Professor with the Institute of Applied Physics, University of Electronic Science and Technology of China (UESTC), Chengdu, China. From 1992 to 1993, he was a Visiting Researcher with the Department of Electrical and Computer Engineering, University of California at Berkeley, Berkeley, CA, USA. From 1993 to 1998, he was a Full Professor with the Institute of Applied Physics, UESTC. He was a Visiting Professor with the Electrical Engineering Department, University of Waterloo, Waterloo, ON, Canada, from February 1998 to May 1998. From 1996 to 1997, he was the Vice Chairman of the Institute of Applied Physics, UESTC, where he was the Chairman of the Institute from 1997 to 1998. From 1998 to 2007, he was with Blackberry Ltd., Waterloo, ON, Canada, first as a Senior Scientist with the Radio Frequency Department, and then the Director of the Advanced Technology Department. Since 2010, he has been a National Distinguished Professor with Fudan University, Shanghai, China, and the Nanjing University of Information Science and Technology (NUIST), Nanjing, where he is currently the Director of the Research Center of Applied Electromagnetics. He has authored over 100 journal publications and *Foundations for Radio Frequency Engineering* (World Scientific, 2015), *Foundations of Applied Electrodynamics* (Wiley, 2010), *Advanced Electromagnetic Field Theory* (China: National Defense Publishing House, 1999), and *Modern Methods for Electromagnetic Computations* (China: Henan Science and Technology Press, 1994). He holds more than 40 patents. His current research interests include microwave theory and techniques and antennas and wave propagation.